

Author's response

We thank the anonymous referees for their comments. We have addressed their concerns and have rewritten the manuscript. Our responses to the referees, a list of the changes made, and the marked-up version of the manuscript follows.

Interactive comment on “The response of tropical precipitation to Earth’s precession: The role of fluxes and vertical stability”, reply to referee 1

Chetankumar Jalihal^{1,3}, Joyce Helena Catharina Bosmans², Jayaraman Srinivasan³, and Arindam Chakraborty^{1,3}

¹Centre for Atmospheric and Oceanic Sciences, Indian Institute of Science, Bangalore, India

²Department of Environmental Science, Radboud University, The Netherlands

³Divecha Centre for Climate Change, Indian Institute of Science, Bangalore, India

Correspondence: Chetankumar Jalihal (jalihal@iisc.ac.in)

1. **General Comments:** The authors thank you for your time and inputs.

2. **Comment:** *Title: fluxes is too general, suggest “energy fluxes” replace fluxes*

Reply: Thank you for the suggestion. We will modify the title to include "energy fluxes".

5

3. **Comment:** *The structures of current manuscript needs to improve and arrange as follows: First part is Introduction, and second part is Model description, and experiments design, methodology. The third part is results shows. Conclusions and discussion appear last part. However, the authors should move most of (maybe all) the formulas in section 2 with a quite clear description. Please re-organize this part.*

10 **Reply:** We will move all the equations to section 2, and explain the equations in more detail.

4. **Comment:** *Table 1 and Table 2 are not very beautiful.*

Reply: We will make better tables for the revised manuscript.

15 5. **Comment:** *All the title of Figurexx is not correct in your figure captions, because one more Arabic number “1” need to remove.*

Reply: This was due to a LaTeX error, which had been fixed in the uploaded version of the discussion paper.

6. **Comment:** *give a regression line for Figure 13 and Figure 14 and then merge into one plot.*

20 **Reply:** Figure 3 and 4 in the discussion paper show the dependence of (P-E) on energy fluxes and stability of the

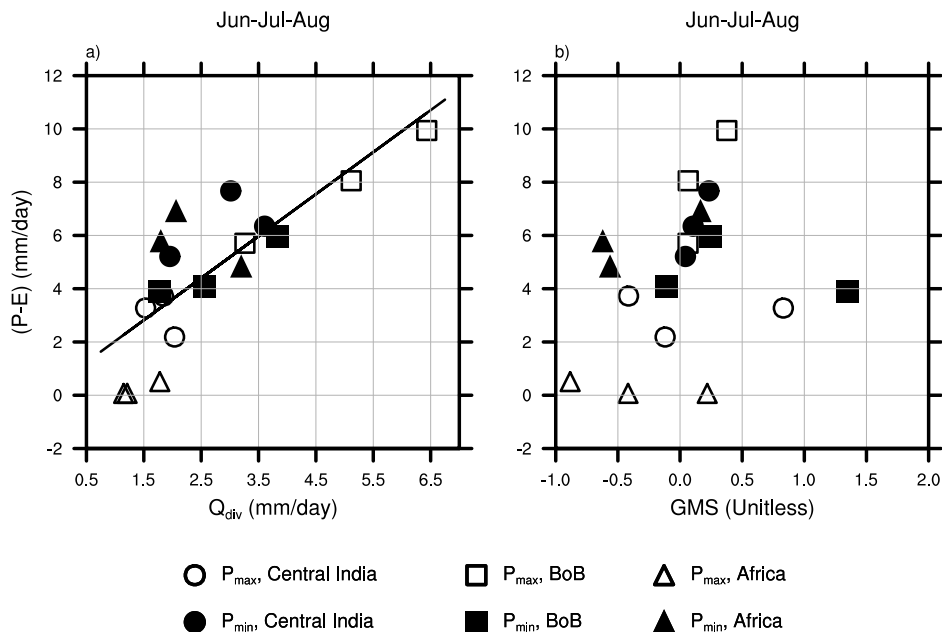


Figure 1. This figure shows the dependence of (P-E) on, (a) Q_{div} (which is sum of all the energy fluxes into the atmosphere) and (b), GMS. The scatter is for three regions: Central India (15°N-25°N; 73°E-83°E), Bay of Bengal (10°N-20°N; 85°E-95°E) and Africa (5°N-15°N; 20°W-25E°). The months JJA have been taken separately. (P-E) is directly proportional to Q_{div} .

atmosphere. Your point is well taken, and the two figures have been combined. (P-E) being a non-linear function of stability, the regression line is not being shown for the scatter of (P-E) and GMS.

7. **Comment:** All the Figures needs to make it more beautiful.

5 **Reply:** We will improve all the figures for the revised manuscript.

Interactive comment on “The response of tropical precipitation to Earth’s precession: The role of fluxes and vertical stability”, reply to referee 2

Chetankumar Jaliha^{1,3}, Joyce Helena Catharina Bosmans², Jayaraman Srinivasan³, and Arindam Chakraborty^{1,3}

¹Centre for Atmospheric and Oceanic Sciences, Indian Institute of Science, Bangalore, India

²Department of Environmental Science, Radboud University, The Netherlands

³Divecha Centre for Climate Change, Indian Institute of Science, Bangalore, India

Correspondence: Chetankumar Jaliha (jaliha@iisc.ac.in)

1. **General Comments:** The authors thank you for your time and inputs.

2. **Comment:** *The structure of the text seems casual. I recommend that the authors put all the methods (including the ITCZ model, equation and decomposition) together. In the result section, it is better to merely show the figure and descriptions. That would help the paper to be easily read.*

Reply: Thank you for the suggestion. We will re-organize the manuscript.

3. **Comment:** *Introduction: there are a lot of modeling studies in this field; however, the authors did not mention them in the introduction. For example,*

Global:

Kutzbach, J., Liu, X., Liu, Z., Chen, G., 2008. Simulation of the evolutionary response of global summer monsoons to orbital forcing over the past 280,000 years. Clim. Dyn. 30, 567-579.

Asia and Africa:

Tuenter, E., Weber, S., Hilgen, F., Lourens, L., Ganopolski, A., 2005. Simulation of climate phase lags in response to precession and obliquity forcing and the role of vegetation. Clim. Dynam. 24, 279-295

Weber, S., Tuenter, E., 2011. The impact of varying ice sheets and greenhouse gases on the intensity and timing of boreal summer monsoons. Quat. Sci. Rev. 30, 469-479.

Shi, Z., Liu, X., Cheng, X., 2012. Anti-phased response of northern and southern East Asian summer precipitation to ENSO modulation of orbital forcing. Quat. Sci. Rev. 40, 30-38.

Caley, T., Roche, D.M., Renssen, H., 2014. Orbital Asian summer monsoon dynamics revealed using an isotope-enabled global climate model. *Nat. Commun.* 5, 5371. <http://dx.doi.org/10.1038/ncomms6371>.

Shi, Z., 2016. Response of Asian summer monsoon duration to orbital forcing under glacial and interglacial conditions: implication for precipitation variability in geological records. *Quat. Sci. Rev.* 139, 30-42

5 **Reply:** Thank you for these references. We will include them in the introduction.

4. **Comment:** Experiments: Only two sensitivity runs are conducted in this study. The authors said the differences between P_{max} and P_{min} scenarios “has a similar spatial precipitation response as observed in MidHolocene, but with higher amplitude”. In actual, there is certain contribution from obliquity in the MH-PI difference. I know in Bosmans et al (2015), there are already obliquity-linked experiments. Why do the authors not give results for the obliquity in this study? In my opinion, it is also important.

10 **Reply:** It is true that the Mid-Holocene response will have contributions from obliquity. However, the obliquity in Mid-Holocene is only 0.66° higher than PI. Hence, its contribution is much less in comparison to that of precession.

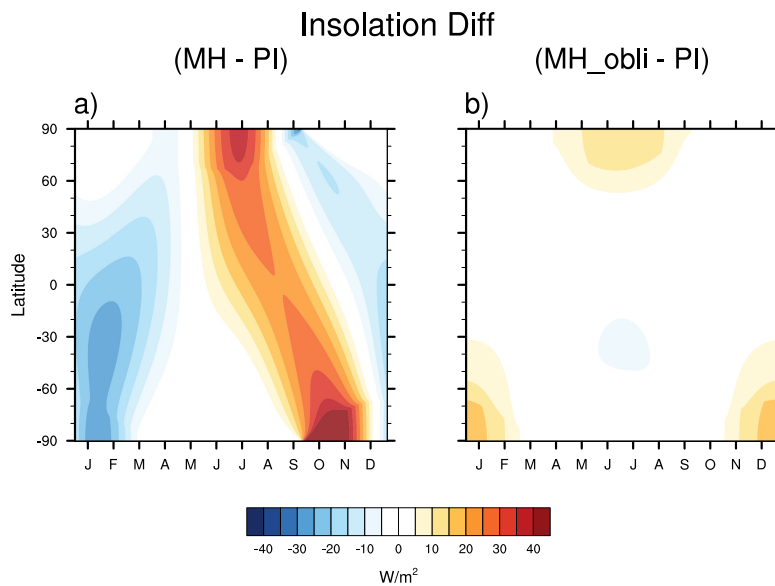


Figure 1. This figure shows that the contribution from tilt to the total insolation change is much smaller in comparison to that from precession. The difference in insolation between, **a)** MH and PI, **b)** MH (obliquity only) and PI.

15 Our analysis is still valid for MH. It is discussed in detail in the section **Results and Discussion-1.1** of this document. The asymmetric precipitation response over India and Bay of Bengal is driven by the same mechanism, in MH and P_{min} .

Obliquity has a much smaller forcing than precession. The land-ocean asymmetric response in tropical precipitation still exists, albeit much weaker at the regional scale. The mechanisms governing these changes are different and hence were not included in the manuscript. **Results and Discussion section 1.2** here, has the relevant discussion.

5. **Comment:** Results: From figure 5 and 6, I can see the distinct response of land and ocean precipitation, but it is also significantly negative over northwestern Pacific besides the Bay of Bengal. This indicates that the East Asian/Northwestern Pacific summer precipitation is also typical for the proposal of this paper. I recommend the authors to add additional analyses on this region and compare the results to those over the Bay of Bengal.

Reply: The response of East Asian/Northwestern Pacific precipitation is shown in the following figure. It will be included in the revised manuscript.

10

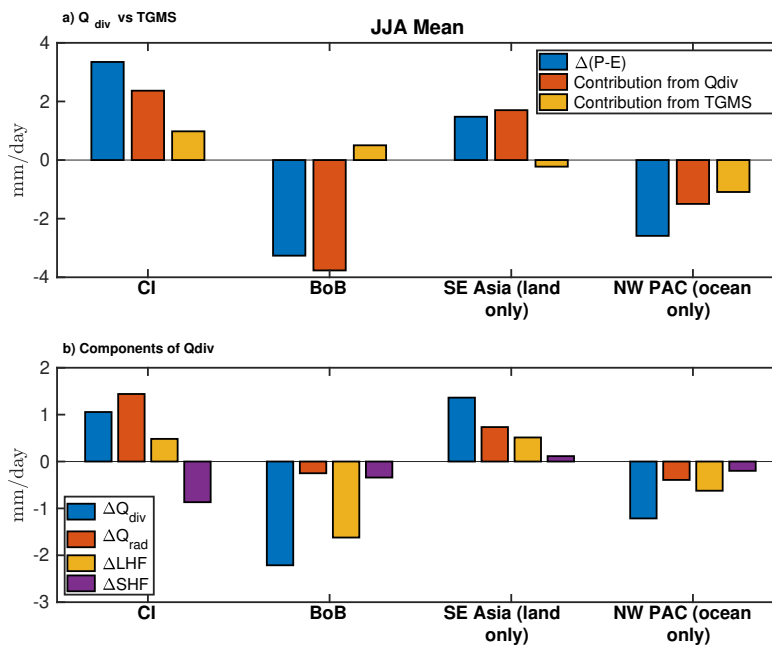


Figure 2. For the extreme precession experiments (.viz. P_{min} and P_{max}), the bar chart shows, **a)** the relative contribution of Q_{div} and TGMS to the changes in (P-E) and, **b)** the changes in the various fluxes contributing to Q_{div} . Here Q_{div} is the sum of all the fluxes at the surface and top of atmosphere, Q_{rad} is the sum of all the radiation fluxes (top and bottom of atmosphere), LHF and SHF are the latent and sensible heat fluxes. ($Q_{div} = Q_{rad} + LHF + SHF$). **CI:** Central India (15° , $25^{\circ}N$; 73° , $83^{\circ}E$) **BoB:** Bay of Bengal (10° , $20^{\circ}N$; 85° , $95^{\circ}E$) **SE Asia:** South East Asia (0° , $25^{\circ}N$; 100° , $125^{\circ}E$)

Figure (2a), shows that the dominant reason for the changes in (P-E) between P_{min} and P_{max} , is Q_{div} for all the four regions chosen. The land regions (Central India and South East Asia) show an increase in Q_{div} (and hence in (P-E)), while over the oceanic regions (BoB and NW Pacific) Q_{div} (and hence (P-E)) decreases. The increased insolation drives the positive changes in Q_{div} over land regions, whereas the decrease in LHF is the main cause of decrease in Q_{div} over

oceanic regions (Figure 2b). This decrease in the surface latent heat fluxes over the North-West Pacific is due to the reduction in wind speeds. This in turn, is a response to the convective heating of atmosphere over the West Equatorial Indian ocean and the Red Sea. This is the same reason why wind speed over the Bay of Bengal reduces (discussed in detail in the discussion paper).

5 1 Results and Discussions

1.1 (P_{\min} - P_{\max}) vs (MH-PI):

In this section, we have discussed the similarities between the sets of experiments (P_{\min} , P_{\max}) and (MH, PI). All four of these experiments used the model EC-Earth. The details of the experiments can be found in (Bosmans et al., 2012, 2015). Both the sets of simulations exhibit a land-ocean asymmetry in the response of precipitation to orbital forcings. The amplitude of the response is nearly a third in the (MH-PI) in comparison to that of (P_{\min} - P_{\max}) (Figure 3). Figure 4 shows the spatial response of (P-E) and Q_{div} . For MH, the response is quite similar in pattern to P_{\min} , but of a smaller amplitude. There are some differences at the regional scale. This could be due to the effect of obliquity. However, the analysis that we have used in the discussion paper can still be used. The India-Bay of Bengal land-ocean asymmetry is due to the same mechanism in both MH and P_{\min} .

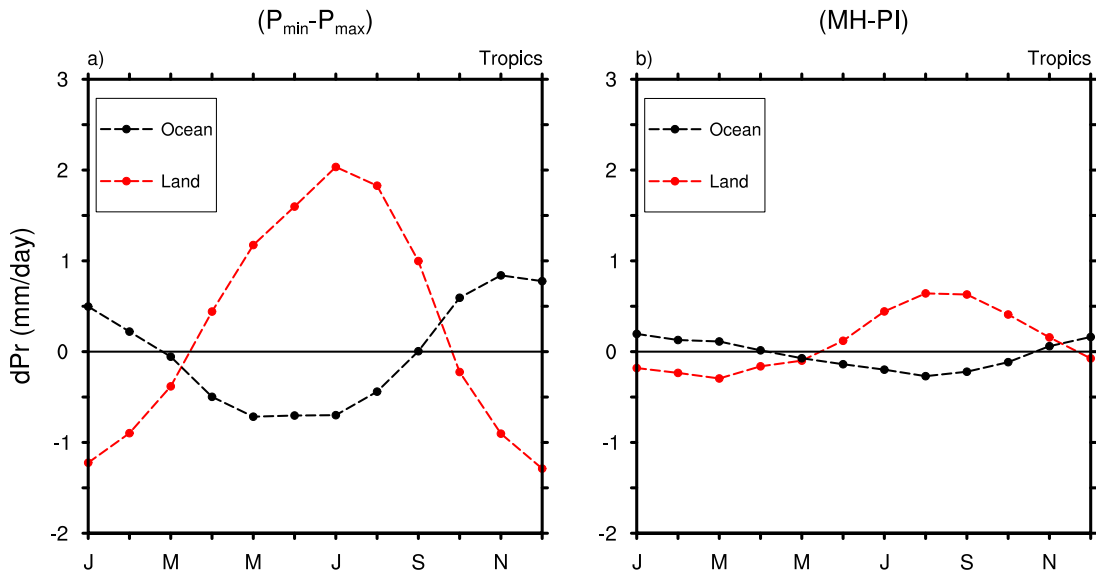


Figure 3. Seasonal cycle of the change in precipitation over all the tropical land and ocean taken separately, for **a)** (P_{\min} - P_{\max}) and, **b)** (MH-PI).

JJA mean

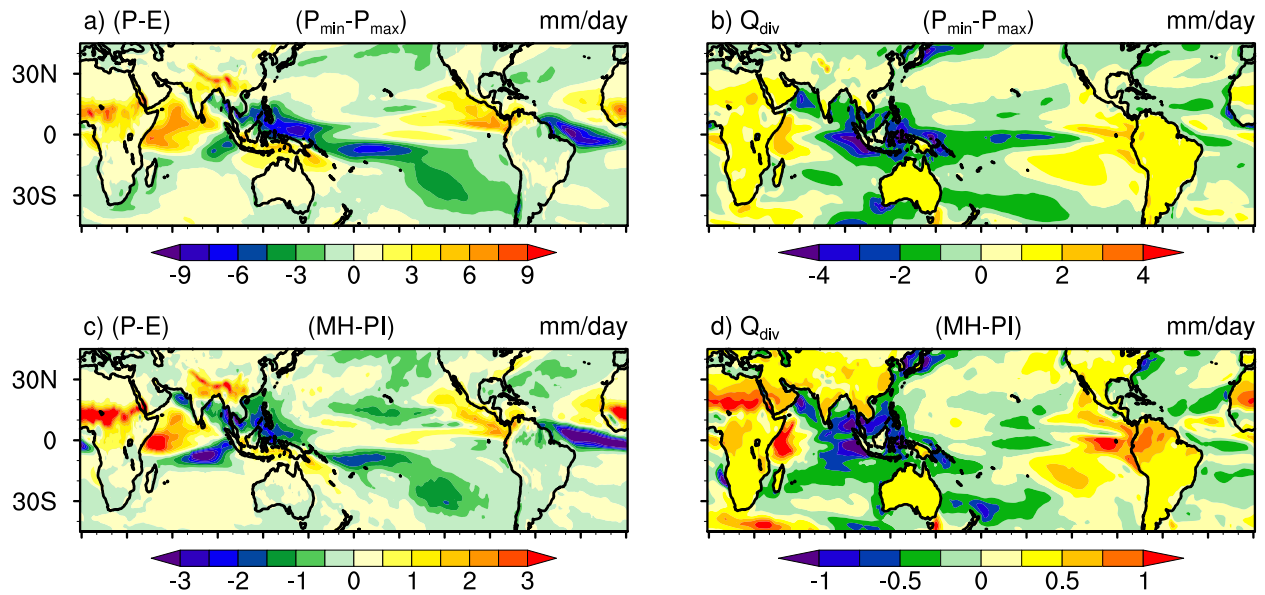
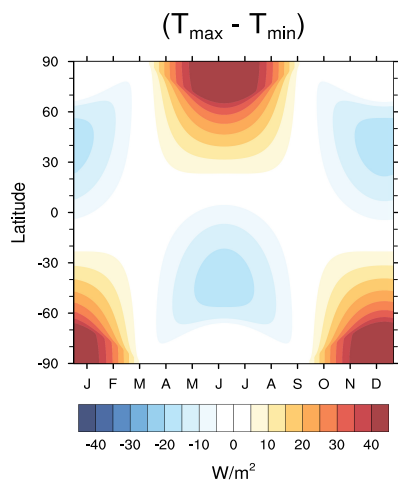


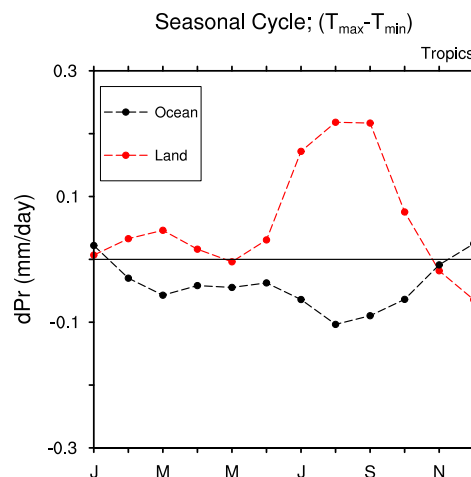
Figure 4. Spatial patterns of the changes in (P-E) (left panel) and Q_{div} (right panel), averaged over JJA. The top panel is for $(P_{min}-P_{max})$ and the bottom panel is for (MH-PI). There is a remarkable spatial coherence, but with a different magnitude.

1.2 Obliquity experiments:

In this section, we have discussed the response of tropical precipitation to obliquity forcing. For these experiments eccentricity was set to zero (circular orbit). The maximum and minimum obliquity experiments (T_{max} and T_{min}) have a tilt of 24.45° and 22.08° , respectively. Further details of the experiments can be found in (Bosmans et al., 2015). Figure 5a shows the difference in insolation between the two obliquity experiments. The obliquity forcing is much smaller than the precessional forcing. However, there still exists a land-ocean asymmetry in the response of tropical precipitation, though of much smaller magnitude (Figure 5b).



(a) Difference in insolation for the two obliquity experiments, T_{\max} and T_{\min} .



(b) Seasonal cycle of the change in precipitation over all of tropical land and ocean taken separately.

Figure 5. Figures showing the obliquity forcing and the precipitation response.

The spatial patterns of the response of (P-E) are in general similar to that of precession (Figure 6). There are however, some regional differences. Using equation 13 of the discussion paper to identify the cause of these changes, reveals a much different mechanism than that for precession. For example, over Central India the changes in (P-E) is due to Q_{div} in the precession experiments (Figure 2a) and due to TGMS in the obliquity experiments (Figure 7a). Even though over BoB, Q_{div} causes a decrease in (P-E) for both precession and obliquity experiments, Q_{div} decreases for different reasons. Precessional forcing causes winds to decrease, which reduces latent heat fluxes. Winds (and hence latent heat flux) also decrease in the obliquity experiments, but the decrease is not large enough. Hence, the changes in net radiation fluxes (Q_{rad}) become equally important (Figure 8f).

$$(T_{\max} - T_{\min})$$

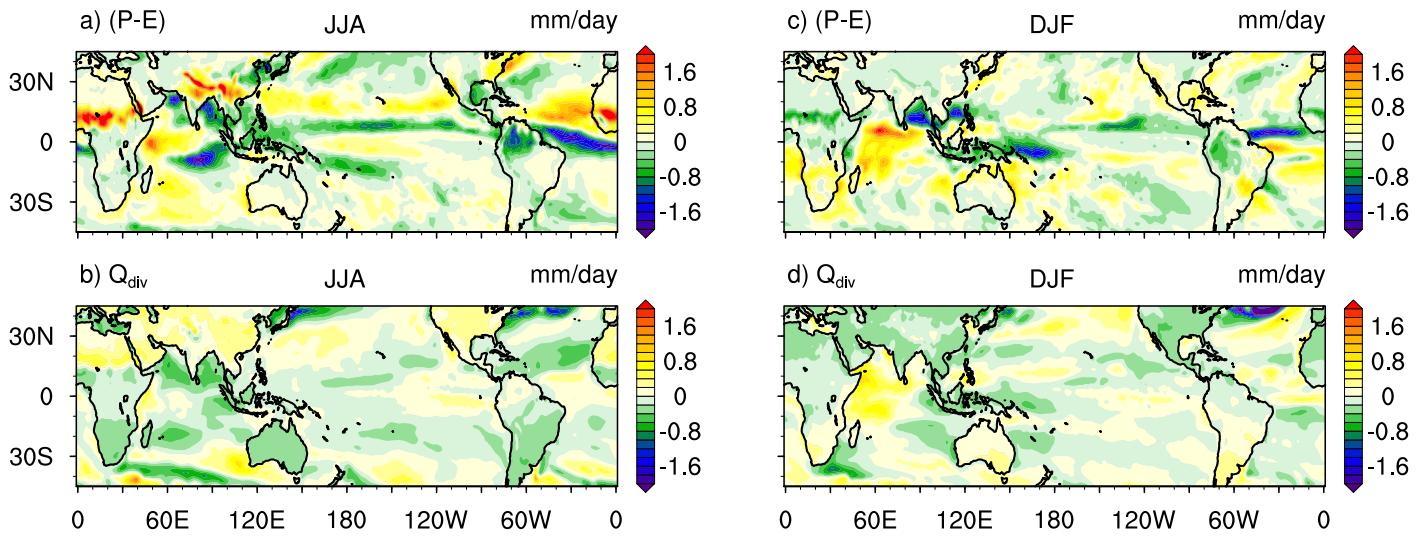


Figure 6. Spatial variation in (P-E) (top panel), and Q_{div} (bottom panel), averaged over the months JJA (left panel) and DJF (right panel).

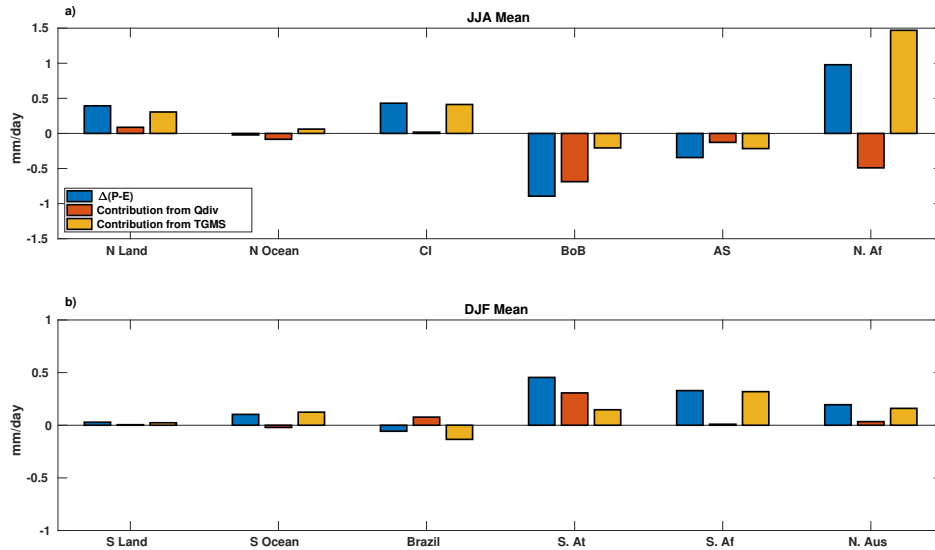


Figure 7. The bar chart shows the relative contribution of Q_{div} and TGMS to the changes in (P-E) for the, (a) northern summer, and (b) southern summer. **N. Land:** Northern Tropics (land only) ($0^{\circ}\text{N}-30^{\circ}\text{N}$; $0^{\circ}\text{E}-360^{\circ}\text{E}$); **N. Ocean:** Northern Tropics (ocean only); **CI:** Central India ($15^{\circ}\text{N}-25^{\circ}\text{N}$; $73^{\circ}\text{E}-83^{\circ}\text{E}$); **BoB:** Bay of Bengal ($10^{\circ}\text{N}-20^{\circ}\text{N}$; $85^{\circ}\text{E}-95^{\circ}\text{E}$); **AS:** Arabian Sea ($10^{\circ}\text{N}-20^{\circ}\text{N}$; $60^{\circ}\text{E}-70^{\circ}\text{E}$); **N. Af:** North Africa ($5^{\circ}\text{N}-15^{\circ}\text{N}$; $20^{\circ}\text{W}-0^{\circ}\text{E}$); **S. Land:** Southern Tropics (Land only) ($30^{\circ}\text{S}-0^{\circ}\text{N}$; $0^{\circ}\text{E}-360^{\circ}\text{E}$); **S. Ocean:** Southern Tropics (Ocean only) ($30^{\circ}\text{S}-0^{\circ}\text{N}$; $0^{\circ}\text{E}-360^{\circ}\text{E}$); **Brazil:** ($20^{\circ}\text{S}-10^{\circ}\text{S}$; $70^{\circ}\text{W}-50^{\circ}\text{W}$); **S. At:** South Atlantic ($20^{\circ}\text{S}-10^{\circ}\text{S}$; $30^{\circ}\text{W}-0^{\circ}\text{E}$); **S. Af:** South Africa ($20^{\circ}\text{S}-10^{\circ}\text{S}$; $15^{\circ}\text{E}-35^{\circ}\text{E}$); **N. Aus:** North Australia ($25^{\circ}\text{S}-15^{\circ}\text{S}$; $130^{\circ}\text{E}-140^{\circ}\text{E}$)

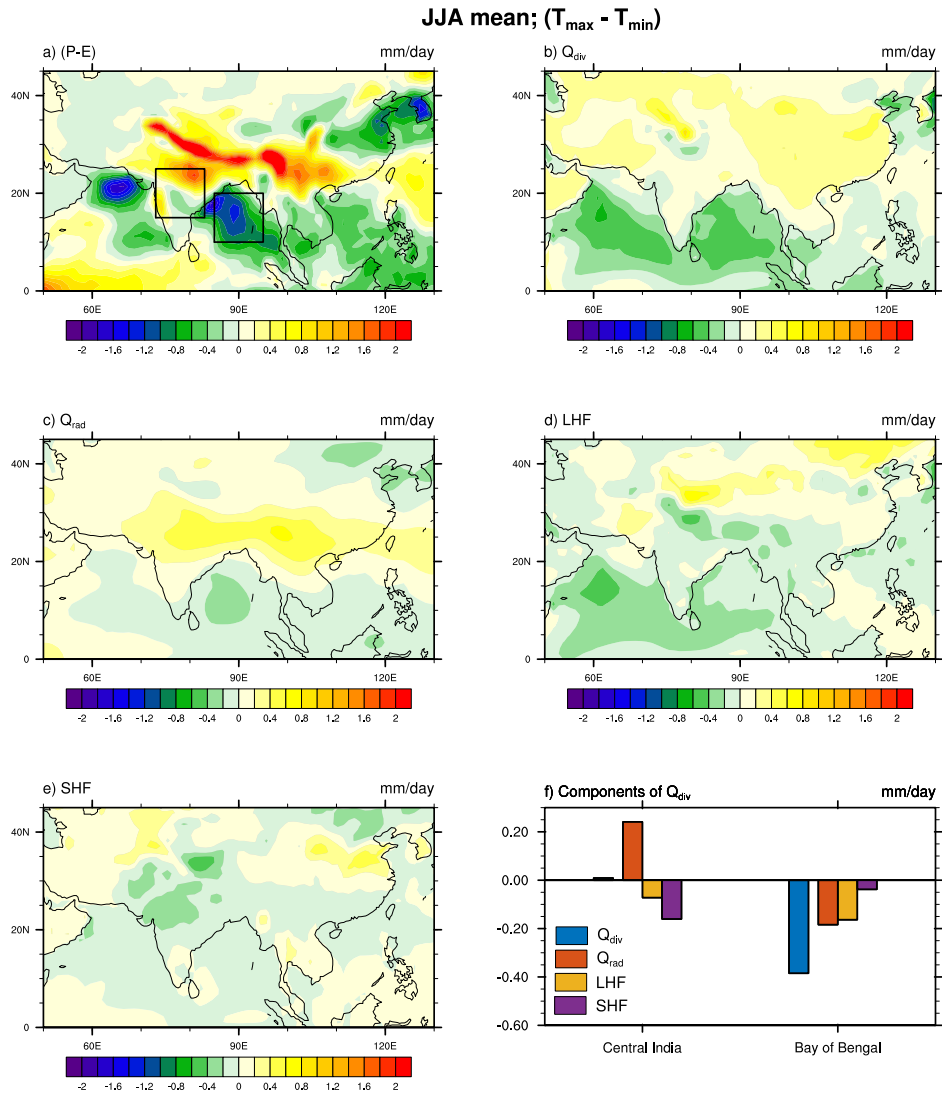


Figure 8. JJA mean difference between P_{\min} and P_{\max} for, **a)** (P-E), **b)** Q_{div} , **c)** Q_{rad} (sum of all radiation fluxes), **d)** Latent Heat Fluxes, **e)** Sensible Heat Fluxes, **f)** the components of Q_{div} .

References

- Bosmans et al.: Monsoonal response to mid-holocene orbital forcing in a high resolution GCM, *Climate of the Past*, 8, 723, 2012.
- Bosmans, J., Drijfhout, S., Tuenter, E., Hilgen, F., and Lourens, L.: Response of the North African summer monsoon to precession and obliquity forcings in the EC-Earth GCM, *Climate dynamics*, 44, 279–297, 2015.

List of relevant changes made:

1. We have modified the title to include the word "energy".
2. The current affiliation of one of the co-authors has been specified.
3. We have moved all the equations to section 3.
4. All the figures and tables have been improved. We have combined the figures 3 and 4 of the discussion paper into one figure and we have shown a regression line.
5. We have restructured the text.
6. We have included all the references suggested by the anonymous referee#2. We also added references that were relevant for the restructured text.
7. Discussion on the impact of Mid-Holocene and obliquity forcing on the tropical monsoon is provided in the discussion section and the supplementary material.
8. A subsection discussing the impacts of precession on the East Asian/Northwestern Pacific summer precipitation is included.
9. Abstract and introduction have been rewritten.
10. Appendix has been moved into the result section.
11. The "Discussion and conclusion" section has been modified substantially.

The response of tropical precipitation to Earth's precession: The role of energy fluxes and vertical stability

Chetankumar Jalihal^{1,3,2}, Joyce Helena Catharina Bosmans^{2,3,4,a}, Jayaraman Srinivasan^{3,2}, and Arindam Chakraborty^{1,3,2}

¹Centre for Atmospheric and Oceanic Sciences, Indian Institute of Science, Bangalore, India

^{3,2}Divecha Centre for Climate Change, Indian Institute of Science, Bangalore, India

³Previously at: Faculty of Geosciences, Utrecht University, the Netherlands

⁴Previously at: Royal Netherlands Meteorological Institute (KNMI), the Netherlands

^{2a}Now at: Department of Environmental Science, Radboud University, the Netherlands

Correspondence: Chetankumar Jalihal (jalihal@iisc.ac.in)

Abstract.

The changes in Earth's precession have an impact on the tropical precipitation. ~~These changes have been ascribed~~ This has been attributed to the changes in solar radiation at the top of the atmosphere, ~~but this~~. The primary mechanism that has been proposed is the change in thermal gradient between the two hemispheres. This may be adequate to understand the zonal mean
5 changes but cannot explain the variations ~~in precipitation over oceans. Using energy and moisture budget equations we have shown that the surface energy fluxes~~, as well as vertical stability, have to be taken into consideration along with insolation, to explain these changes in precipitation. ~~Energy fluxes explain most of the changes in precipitation, when looking at the mean response over the tropics. However, there are regions like the Arabian sea and Africa where stability change is the main cause of change in precipitation. Hence, insolation cannot be thought of as the sole driver of~~ between land and oceans. We have used
10 a simple model of the intertropical convergence zone (ITCZ) to unravel how precipitation changes with precession. Our model attributes the changes in precipitation to the changes in energy fluxes and vertical stability. We include the horizontal advection terms in this model, which were neglected in the earlier studies. The final response of the land and oceans is a result of complex feedbacks triggered by the initial changes in the insolation. We find that the changes in precipitation over the land are mainly driven by changes in insolation, but over the oceans, precipitation changes on account of changes in surface fluxes and vertical
15 stability. Hence insolation can be a trigger for changes in precipitation on orbital timescales, but surface energy and vertical stability ~~should also be considered when looking at oceans or smaller land regions. The decrease in precipitation over the Bay of Bengal, with~~ play an important role too. The African monsoon intensifies during a precession minimum (higher summer insolation, ~~has been shown to be~~). This intensification is mainly due to the ~~decrease in surface latent heat fluxes. This is a consequence of the remote response of the atmosphere~~ changes in vertical stability. The precipitation over the Bay of Bengal
20 decreases for minimum precession. This is on account of a remote response to the enhanced ~~latent convective~~ heating to the west of Bay of Bengal. This weakens the surface winds and thus leads to a decrease in ~~wind speed over the Bay of Bengal and hence reduces the total column energy available for convection~~ the surface latent heat fluxes and hence the precipitation.

1 Introduction

~~Using speleothem records, past studies have shown~~ The most dominant temporal mode in insolation and tropical precipitation is the 23,000-year precession cycle of the Earth (Berger, 1978; Kutzbach, 1981; Pokras and Mix, 1987). Both proxy (Wang et al., 2007, 2008) and model (Kutzbach, 1981; Kutzbach et al., 2008; Tuenter et al., 2005; Weber and Tuenter, 2011; Caley et al., 2014; Shi, 2016) based studies suggest that the intensity of ~~monsoon is directly proportional~~ monsoons have varied in proportion to insolation on orbital timescales (~~Wang et al., 2007, 2008; Cruz Jr et al., 2005~~). ~~The model-based studies suggest, however, that while this is true over land, the precipitation over tropical oceans is in general, inversely related to insolation (Clement et al., 2004; Tuenter et al., 2003; 2004). For example, the summers of Mid-Holocene (MH), had about 20 W/m² more insolation over India, than the present-day summer. An increase in summer rainfall can be found in the proxies (Ramesh, 2001; Patnaik et al., 2012; Zhang et al., 2016) The simulations of the MH monsoon by climate models indicate that the precipitation over Bay of Bengal (BoB) was less (Hsu et al., 2010; Bosmans et al., 2012; Zhao and Harrison, 2012). The India-BoB asymmetry, is a regional manifestation of the land-ocean asymmetry in the response of precipitation to changes in the Earth's precession. When changes in precession increase the insolation in the northern hemisphere, the zonal mean precipitation band shifts northward on account of the increase in thermal gradient between the two hemispheres (Donohoe et al., 2013; Schneider et al., 2014; Kang et al., 2008). This mechanism cannot explain the longitudinal changes in precipitation (Mohtadi et al., 2016). The simulation of climate models shows that precipitation over land and oceans respond differently to precessional forcing (Clement et al., 2004; Tuenter et al., 2003; 2004). This has been observed in the idealized as well as realistic precession experiments with climate models (e.g., Braconnot et al., 2008; Zhao et al., 2008).~~

~~This has been explained~~ It is attributed to the land-sea contrast theory, in the previous studies ~~using the land-sea thermal contrast theory of the monsoon (Zhao and Harrison, 2012; Bosmans et al., 2012). According to this theory, with increased insolation (Zhao and Harrison, 2012; Bosmans et al., 2012). The land warms more than the surrounding ocean, because of due to its lower thermal inertia. This increases the land-sea thermal contrast in surface temperature. However, the thermal contrast~~ Hence a low pressure develops over land and a monsoon circulation is established. The increase in insolation leads to deeper thermal lows over land, which enhance the onshore flow of moisture-laden winds. This leads to stronger ascent over land and an increase in precipitation. This thermal contrast, however, disappears after the onset of monsoon due to the cooling of land by precipitation and cloud cover. In fact, in good monsoon years ~~have a lower~~, the land surface temperature is lower (Gadgil, 2018).

~~The other mechanism that has been proposed is the slow-ocean-response theory (Braconnot et al., 2000; Hsu et al., 2010). The ocean, due to its higher heat capacity, takes about a month or two to respond to the insolation forcing. However, there are still many oceanic regions where, precipitation responds differently. This indicates that local processes are dominant in those regions. Thus the slow-ocean response while true in general, may not explain precipitation response in small basins like the Bay of Bengal.~~

Some studies have used the changes in energy balance to ~~explain~~ understand the response of precipitation to precession (Braconnot et al., 2008; Hsu et al., 2010; Merlis et al., 2013; Chamales, 2014; Battisti et al., 2014). ~~While Braconnot et al. (2008)~~

suggested a possible connection between changes in precipitation and changes in divergence of Moist Static Energy (MSE), Chamales (2014) and Merlis et al. (2013) have shown how they are connected using a theoretical framework. The analysis done by Merlis et al. (2013) is for the zonal mean, and this does not reflect the actual conditions in a full General Circulation Model (GCM) with continents. Hsu et al. (2010) found in their model of intermediate complexity that the changes in vertical velocity, which are in turn a response to changes in Braconnot et al. (2008) suggested that the net energy in the atmosphere over land and adjacent oceans changes due to precession. The atmosphere then acts to redistribute the excess energy, thereby setting up a land-ocean difference in precipitation. Hsu et al. (2010) showed that the precipitation changes due to precession are related to the changes in the total column energy drive the changes in precipitation. This is again a tropical mean picture and regional response might be different from the tropical mean response. Also, a quantitative estimate of the parameters governing , which drives changes in vertical velocity. Chamales (2014) on the other hand has argued that the stability over oceans changes, whereas land regions respond by transporting the excess moist static energy. These are, however, generalizations for the entire tropics. The role of local processes and feedbacks might be important in driving regional changes in precipitation is missing. Battisti et al. (2014) focused on the asymmetry between central India and Bay of Bengal, and . Thus, individual regions need to be studied separately, to understand the cause of the changes. For example, Battisti et al. (2014) suggested that higher summer insolation causes the near surface energy to migrate leads to a migration of the near-surface moist static energy from the Bay of Bengal to India. But as shown in the appendix A, our climate model does not show such a migration in near surface energy. We propose an alternative model based on total energy in a column and stability of the column to explain the changes in precipitation in all regions of the tropics in response to changes in Earth's precession, before the onset of monsoon. They argued that hence the precipitation centroid shifts to India.

In this paper we have used We have used time-slice experiments in a high-resolution , state-of-the-art fully coupled model GCM EC-Earth (Bosmans et al., 2015). This GCM was run in two orbital configurations , which correspond to the extremes in precession -(Fig. 1). The advantage of doing this is that , it has a similar spatial precipitation response as observed in MH, but with higher amplitude. This the amplitude of the response is large, while the spatial pattern is similar to a simulation of realistic precession such as MH. In this paper, we propose a simple model based on the conservation of moisture and moist static energy, to interpret the changes in precipitation between the precession extremes. The paper is organized as follows. The next section describes the model and the experimental setup. Section 3 outlines the derivation of a simple model for the Inter Tropical Convergence Zone-intertropical convergence zone (ITCZ) that we have used to interpret the results. We have used this simple ITCZ model to understand the factors leading to the shift in precipitation between land and oceans, at the regional scale. The results are described in section 4 followed by discussion and conclusions a discussion where we have examined the precipitation response to MH and Obliquity forcing with the help of the simple ITCZ model.

2 Model and experimental details

EC-Earth is a fully coupled ocean-atmosphere GCM , (Hazeleger et al., 2010, 2012). The (Hazeleger et al., 2010, 2012). We have used the model version 2.2 where, . The Integrated Forecasting System (IFS) is was the atmospheric component was used.

~~It has a spectral resolution of~~. The spectral resolution was T159 (roughly $1.125^{\circ} \times 1.125^{\circ}$) with 62 vertical levels. The convective scheme Bechtold et al. (2008) ~~is was~~ used along with the Balsamo et al. (2009) land surface scheme H-TESSSEL, including surface runoff. The ~~version 2 of~~ Nucleus for European Modeling of the Ocean (NEMO) ~~forms~~, version 2 was the ocean component. ~~It has a horizontal resolution of~~ The horizontal resolution was 1° with 42 vertical levels (Madec, 2008; 5 Sterl et al., 2012). NEMO includes sea-ice model LIM2. OASIS3 coupler Valcke and Morel (2006) couples the ocean, sea-ice, land, and atmosphere. EC-Earth performs well for the present day when compared to CMIP3 models in terms of climatology as well as inter-annual, spatial and temporal variability (Hazeleger et al., 2010, 2012).

~~Earth's precession with a period of 23,000 years, is the most dominant mode in insolation as well as in tropical precipitation.~~ The two precession extremes, Precession minima: P_{\min} and Precession maxima: P_{\max} , correspond to summer solstice at perihelion and winter solstice at perihelion respectively (~~Figure 1~~ Fig. 1). Table ~~1~~, 1 shows the orbital configurations used. This ~~causes~~ leads to a stronger seasonal cycle in the Northern Hemisphere (NH) and a weaker seasonal cycle in Southern Hemisphere (SH), ~~in P_{\min}~~ in P_{\min} (~~Figure 2~~). ~~The opposite occurs during a~~ Fig. 2. On the other hand, the seasonal cycle is weaker in the NH and stronger in the SH in P_{\max} .

The model is run separately for each of the orbital configurations. The length of each simulation is 100 years, with the first 50 15 years being considered as spin-up. ~~The~~ We have used the climatology of the last 50 years ~~are used to generate climatology. All analysis has been done with this climatological data, for all our analysis.~~ The orbital parameters remain constant throughout the simulation. All other boundary conditions (e.g. the solar constant, greenhouse gas ~~concentrations~~ concentrations, orography, ice sheets, vegetation) were kept constant at the pre-industrial levels. Vernal equinox has been fixed at 21st March, and the present-day calendar is used. ~~But since~~ Since the length of the season and the dates of equinoxes change along the ~~precession~~ precession 20 precession cycle, the autumn equinoxes do not coincide. This is known as the ~~Calendar Effect~~ "Calendar Effect". It introduces some errors due to the phasing of insolation. We do not make any corrections in order to be consistent with previous studies. ~~For further~~ Further details about the experiments ~~see are provided in~~ Bosmans et al. (2015).

3 A simple model for ITCZ

Hadley cell is a thermally direct, overturning circulation in the tropics. It takes energy away from the tropics and transports 25 it towards the poles. The Hadley cell has a rising branch in the deep tropics and a descending branch in the extra-tropics. This leads to moisture convergence near the rising branch. ITCZ coincides with the rising branch of the Hadley cell, and is responsible for the zone of heaviest precipitation in the tropics. ~~Since, the Hadley cell is governed by energy and leads to moisture convergence, the characteristics of~~ The characteristics of the ITCZ can be described by using the conservation equations for Moist Static Energy (MSE) and moisture. Using this approach, Neelin and Held (1987) proposed a simple model 30 for ITCZ in terms of net energy input into the atmosphere and vertical stability. This is a diagnostic model, that has been used to explain variations in rainfall due to global warming (Chou and Neelin, 2004; Chou et al., 2006) and the ~~impact~~ impacts of aerosols (Chou et al., 2005). In this section, we have discussed this simple model in detail.

The equations 1 and 2 correspond to the conservation of MSE and moisture in a vertical column of the atmosphere. Refer to Neelin and Held (1987) for further details. The first term in both the equations is horizontal divergence, with the second term being the vertical divergence of MSE and moisture fluxes respectively.

The quantities on the right-hand side are the sum of all sources and sinks. Further details on the derivation of equation 1. Eq. 1 can be found in Neelin and Held (1987). The time derivatives have been dropped in these equations because the climate is assumed to be in a steady state. The angle brackets ($\langle \rangle$) indicate vertical integral.

$$\langle \nabla \cdot m\mathbf{U} \rangle + \left\langle \frac{\partial m\omega}{\partial p} \right\rangle = Q_{div} \quad (1)$$

$$\langle \nabla \cdot q\mathbf{U} \rangle + \left\langle \frac{\partial q\omega}{\partial p} \right\rangle = E - P \quad (2)$$

$$\langle A \rangle = - \int_{P_b}^{P_t} A \frac{dp}{g} \quad (3)$$

where

P - Precipitation (mm/day)

E - Evaporation (mm/day)

Q_{div} - Total Column Energy, i.e. the sum of all the energy fluxes into the atmosphere at the top and bottom of the atmosphere. (Eq. 4). (in mm/day; taking the latent heat of vaporization as $2.26 \times 10^6 \text{ J kg}^{-1}$ we get $1 \text{ mm/day} = 26.16 \text{ W/m}^2$). Over land since the storage term is small, the sum of all the fluxes of energy at the surface is small. Hence, Q_{div} is mainly governed by the fluxes at the Top of Atmosphere (TOA). However, over oceans the contribution of surface fluxes is large.

q - specific humidity (kg/kg)

m - Moist Static Energy (J kg^{-1}), which is the sum of internal energy, potential energy and moist energy ($C_p T + gZ +$

$L_v q$)

P_b - Pressure at the bottom of the atmospheric column (Pa)

P_t - Pressure at the top of the atmospheric column (Pa)

g - acceleration due to gravity (m s^{-2})

The full equation for Q_{div} is:

$$Q_{div} = \underbrace{LHF + SHF + Net_Sfc_Rad}_{\text{bottom fluxes}} + \underbrace{Net_TOA_LW + Net_TOA_SW}_{\text{TOA Fluxes}} \quad (4)$$

Where,

LHF : Surface Latent Heat Flux (mm day⁻¹)

SHF : Surface Sensible Heat Flux (mm day⁻¹)

Net_Sfc_Rad : Net Surface Radiation (Long wave + Short wave) (mm day⁻¹)

5 Net_TOA_LW : Net Top Of Atmosphere Long wave radiation (mm day⁻¹)

Net_TOA_SW : Net Top Of Atmosphere Short wave radiation (mm day⁻¹)

Clubbing all the radiation fluxes together into one quantity ' Q_{rad} ', we get:

$$Q_{div} = LHF + SHF + Q_{rad} \quad (5)$$

10 Assuming $\omega = 0$ at the top as well as the surface, leaves us with the horizontal terms only. The governing equations can be combined and simplified (equation 4)-as:

$$P - E = \frac{Q_{div}}{GMS} \quad (6)$$

$$GMS = \frac{m_1 - m_2}{L_v(q_2 - q_1)} \quad (7)$$

$$m_1 = \frac{\int_{P_t}^{P_m} m \nabla \cdot U dp/g}{\int_{P_t}^{P_m} \nabla \cdot U dp/g} \quad (8)$$

$$15 \quad m_2 = \frac{\int_{P_m}^{P_b} m \nabla \cdot U dp/g}{\int_{P_m}^{P_b} \nabla \cdot U dp/g} \quad (9)$$

where, Where, GMS is the ~~Gross Moist Stability~~ gross moist stability, as obtained by taking the ratio of the ~~equations Eqs.~~ 2.11 and 2.12 from (Neelin and Held, 1987). ~~m_1 and m_2~~ m_1 and m_2 are respectively, the total MSE in the upper (mid-troposphere to top) and lower troposphere (surface to mid-troposphere), normalized by the divergence of that layer. Thus, GMS is mainly a function of vertical profiles of MSE. ~~P_m~~ Pressure at and it provides a measure of vertical stratification of the atmosphere. P_m is pressure at the mid-troposphere level. ~~Similarly, q_1 and q_2~~ . Similarly, q_1 and q_2 represent the total moisture in the upper and lower troposphere, normalized by divergence. The mass convergence in the lower troposphere is the same as the

mass divergence in the upper troposphere. ~~Here (Neelin and Held, 1987) assume that the horizontal gradients~~ The horizontal variations of temperature and moisture are assumed to be weak within the tropics. This implies that the horizontal advection of temperature and moisture are small. This simple model attributes the changes in ~~(P-E)~~ $P - E$ to either the changes in total column energy or the vertical stability.

5 Figure ~~3-3a~~ shows a scatter of ~~(P-E)~~ $P - E$ as a function of ~~Q_{div}~~ Q_{div} for the three summer months ~~JJA~~ June, July, and August taken separately. The scatter is made for Central India, ~~BoB~~ the Bay of Bengal and North Africa for each of the precession extremes. We chose these three regions to highlight that neglecting the role of horizontal advection, may not always be appropriate. The plot shows that the two are nearly linear, as ~~predicted~~ indicated by the simple model (~~equation 4~~ Eq. 6). The slight deviations from linearity are due to variations in GMS. As we go from P_{max} to P_{min} (low to high insolation in NH
10 summer months), both ~~Q_{div} and (P-E)~~ Q_{div} and $P - E$ increase over Central India and North Africa (land regions). However, both these quantities decrease over ~~BoB~~ the Bay of Bengal (oceanic region). ~~Being the summer months,~~ Q_{div} The net energy input into the atmosphere and thus, Q_{div} is positive for all these regions during the summer.

~~To further look at the role of GMS we~~ We have shown in figure ~~43b~~, a scatter of ~~(P-E)~~ $P - E$ vs GMS for the same ~~three regions and months~~. ~~There regions~~. The figure shows that there is no definite relation between the two. ~~Based on equation 4, we~~ would expect all positive Equation 6 suggests that all values for GMS ~~since, (P-E) and Q_{div} should be positive since $P - E$ and Q_{div} are both positive~~. ~~But there are some points~~ There are, however, some points in the scatter where GMS is negative. This indicates that the assumption about the horizontal advection ~~terms~~ being small is not always valid. Hence, we ~~need to~~ modify the definition of GMS to include the horizontal advection terms.

By taking the ratio of ~~equations 1 and 2~~ Eqs. 1 and 2, after multiplying ~~equation 2~~ Eq. 2 by L_v (the latent heat of vaporization
20 for water), we get:

$$P - E = \frac{Q_{div}}{TGMS} \quad (10)$$

$$TGMS = \frac{\left\langle \nabla \cdot m\mathbf{U} + \frac{\partial m\omega}{\partial p} \right\rangle}{L_v \left\langle \nabla \cdot q\mathbf{U} + \frac{\partial q\omega}{\partial p} \right\rangle - L_v \left\langle \nabla \cdot q\mathbf{U} + \frac{\partial q\omega}{\partial p} \right\rangle} \left\langle \nabla \cdot m\mathbf{U} + \frac{\partial m\omega}{\partial p} \right\rangle \quad (11)$$

~~Where,~~ Where, TGMS stands for ~~Total~~ total GMS (the term ‘‘Total’’ indicates inclusion of all advection terms). ~~TGMS,~~ has TGMS is based on only one assumption ~~built into it,~~ that the time derivatives of ~~m and q are very small~~ m and q are negligible.
25 This is a good assumption for ~~a steady state climate~~ seasonal mean conditions. TGMS is particularly useful for smaller regions, where horizontal advection can be large. TGMS represents how efficiently an atmospheric column can diverge MSE per unit moisture converged into the column. TGMS is an extension of the concept of GMS, with horizontal advection terms included. This suggests that, along with the ~~vertical profile of MSE, the amount of energy taken out of the column and the amount of moisture going into the column might be important~~. ~~Since we are using climatological data, the errors in energy fluxes and~~ vertical stratification of a column, the lateral transport of MSE and moisture determine the precipitation. A value of TGMS
30

similar in magnitude to GMS indicates that the horizontal transport of MSE is negligible. A change in TGMS between two climates would suggest that the transport of MSE has changed. We have used the ~~calculations of TGMS were significant. Hence, we use the~~ equivalence in ~~equation 1 and 2, Eq. 1 and 2~~ to estimate TGMS. Since ~~our goal is not to estimate the changes in (P-E), P - E~~ but to diagnose the cause of these changes, ~~estimation of TGMS this way, can be justified. there is no~~ need to make an independent estimate of TGMS.

To quantify the relative contribution of Q_{div} and TGMS to the changes in $P - E$, we do the following. Writing Eq. 10 for P_{max} :

$$P - E = \frac{Q}{G} \quad (12)$$

Where P , E , Q , and G are precipitation, evaporation, Q_{div} , and TGMS respectively. Considering P_{max} as the reference case and P_{min} as the perturbed case, we can write the following for P_{min} :

$$(P + \Delta P) - (E + \Delta E) = \frac{Q + \Delta Q}{G + \Delta G} \quad (13)$$

Where Δ represents the perturbation from P_{max} . Now dividing by $P - E$, we get

$$1 + \frac{\Delta(P - E)}{(P - E)} = \frac{1 + \Delta Q/Q}{1 + \Delta G/G} \quad (14)$$

This equation can further be modified as:

$$\underbrace{\frac{\Delta(P - E)}{(P - E)}}_{\text{Change in P-E}} = \underbrace{\frac{\frac{\Delta Q}{Q}}{1 + \frac{\Delta G}{G}}(P - E)}_{\text{Contribution from } Q_{div}} + \underbrace{\frac{\frac{-\Delta G}{G}}{1 + \frac{\Delta G}{G}}(P - E)}_{\text{Contribution from TGMS}} \quad (15)$$

4 Results

In this section ~~we have discussed the relative importance of Q_{div} and TGMS in explaining the changes in (P-E), we have explained the changes in $P - E$ between P_{min} and P_{max} . First we in terms of Q_{div} and TGMS.~~ We start by giving an overview of the entire tropics and then we look at the ~~peculiar case of the Indian subcontinent~~ South Asian monsoon in detail.

4.1 Tropics

4.1.1 Qualitative analysis

Figure 5-4 shows the difference in precipitation between P_{min} and P_{max} ~~averaged over~~ averaged over the tropical land and oceans separately. Precipitation change over the tropical land is out of phase with the changes in precipitation over the oceans.

Amplitude of the change is higher over land than over oceans. ~~Also note that larger change in precipitation~~ Furthermore, over land, ~~occurs during boreal summer when compared to the change is of a higher magnitude during the boreal summer than the austral summer.~~ This implies that the northern hemisphere monsoons are more sensitive to precession than ~~southern monsoons.~~ ~~Since, for both the orbital configurations Vernal equinox occurs on the same date (the southern hemisphere monsoons. The vernal equinoxes during P_{min} and P_{max} occur on the 21st March) of March.~~ Therefore, the difference in insolation between the two cases is very small during March. Hence, ~~the precipitation response is also similar. Therefore the the~~ changes in land and ocean precipitation ~~has have~~ a zero crossing during this month. Since, ~~the quantity of interest to us is (P-E), from here onwards, all of our analysis concerns (P-E) instead of just we are interested in regions where there is moisture convergence, our analysis will focus on $P - E$ instead of precipitation.~~

10 In figure ~~6, is shown a 5,~~ the spatial pattern of the changes in ~~(P-E) and Q_{div}~~ $P - E$ and Q_{div} are shown averaged over JJA (left ~~panels~~ panel) and DJF (right ~~panels~~ panel). First, we discuss the ~~response changes in precipitation~~ during JJA. Most of the land regions in the northern hemisphere show an increase in ~~(P-E) and $P - E$.~~ The African monsoon ~~is much stronger has strengthened substantially~~ in P_{min} with an increase of about 10 mm /day. ~~(P-E) has in general decreased over day⁻¹. $P - E$ has, in general, decreased over the~~ oceans. However, there are many regions over ~~oceans where (P-E) the oceans (e.g., the Arabian~~ Sea) where $P - E$ has increased. ~~Ocean has a much more heterogeneous response in comparison to land. This explains why Hence,~~ the amplitude of the changes in ~~(P-E) $P - E$~~ is small when averaged over all of the tropical oceans (figure 5)-

~~Changes in Q_{div} having a strikingly similar spatial pattern Fig. 4). The changes in Q_{div} have a pattern similar to that of (P-E) $P - E$,~~ with positive values over most of the land regions, and both positive and negative values over ~~the~~ oceanic regions. This ~~shows again is due to the direct relation of (P-E) to Q_{div} between $P - E$ and Q_{div}~~ as suggested by the simple model. ~~However, there are There are, however,~~ some exceptions like the Arabian ~~sea where, Q_{div} has decreased but (P-E) Sea and Africa. Q_{div} has decreased over the Arabian Sea but, $P - E$ has increased. Also the region of maximum increase in (P-E) and Q_{div}~~ The region of the largest increase in $P - E$ and Q_{div} are not co-located over Africa. ~~This is These are~~ on account of the changes in TGMS.

During DJF, P_{min} has lesser insolation (Figure 2 Fig. 2) and correspondingly a decrease in ~~(P-E) and Q_{div}~~ $P - E$ and Q_{div} is seen over ~~the~~ land regions (Figure 6 Fig. 5c and d). ~~Oceans show a heterogeneous response Over oceans, there are regions of both positive and negative changes in $P - E$ during DJF as well. Even though, the The~~ magnitude of changes in Q_{div} are of the same order as in JJA ~~Q_{div} is of a similar order during JJA and DJF. However,~~ the changes in ~~(P-E) are much less in DJF as compared to JJA $P - E$ are larger during JJA compared to DJF.~~

4.1.2 Quantitative analysis

30 To quantify the relative dominance of Q_{div} and TGMS in explaining the changes in (P-E), we do the following. Writing equation 8 for P_{max} :

$$P - E = \frac{Q}{G}$$

where, P, E, Q and G are precipitation, evaporation, Q_{div} and TGMS respectively. Considering P_{max} as the reference case and P_{min} as the perturbed case, we can write the following for P_{min} :

$$\frac{(P + \Delta P) - (E + \Delta E)}{G + \Delta G} = \frac{Q + \Delta Q}{G + \Delta G}$$

Where Δ represents the perturbation from P_{max} . Now dividing by (P-E), we get-

$$1 + \frac{\Delta(P - E)}{(P - E)} = \frac{1 + \Delta Q/Q}{1 + \Delta G/G}$$

This equation can further be modified as:-

$$\underbrace{\Delta(P - E)}_{\text{Change in P-E}} = \underbrace{\frac{\frac{\Delta Q}{Q}}{1 + \frac{\Delta G}{G}}(P - E)}_{\text{Contribution from } Q_{div}} + \underbrace{\frac{-\frac{\Delta G}{G}}{1 + \frac{\Delta G}{G}}(P - E)}_{\text{Contribution from TGMS}}$$

Now we apply the above equation to different regions in In this section, we look at the various terms in Eq. 15 in different regions of the tropics (Figure 7 Fig. 6). The top panel is for regions in the northern hemisphere and the bottom panel is for the southern hemisphere and bottom panels are for the northern and southern hemispheres respectively. The analysis was done for the summer months of the respective hemispheres (JJA for the northern and DJF for the southern hemisphere). The blue stick bar represents the changes in (P-E) $P - E$, whereas the red and orange sticks light red and dark red bars are contributions from Q_{div} Q_{div} and TGMS. Q_{div} Q_{div} explains most of the changes in (P-E) over all of $P - E$ when all the land regions in northern tropics. This is however, a generalization because, the northern tropics are taken together. This need not be true in smaller regions. For example, TGMS contributes most to the changes in (P-E) $P - E$ over Africa. Because of the heterogeneous response of (P-E) over oceans, the fractional change in (P-E) is very small and the contributions from Q_{div} $P - E$ has a different sign over various oceanic regions, the change in $P - E$, averaged over all the tropical oceans is small. The contributions from Q_{div} and TGMS are in opposite directions, thus cancelling almost canceling each other out. BoB shows a decrease in (P-E) most of which is explained by changes in Q_{div} . The contribution from TGMS is, however, slightly higher. The Arabian Sea shows an increase in $P - E$, due to a change in TGMS. The decrease in $P - E$ over the Bay of Bengal is, however, mainly due to changes in Q_{div} with the changes in TGMS being very small.

The southern tropics has a dominant contribution from Q_{div} over both land and oceans. However, some of the regions shown either have an equal contribution from TGMS (In the southern tropics the dominant contribution is from changes in Q_{div} over land and changes in TGMS over oceans. In the case of South Africa and Brazil) or TGMS is the dominant cause changes in TGMS and Q_{div} make an equal contribution. TGMS drives most of the changes in (P-E) (North $P - E$ over northern Australia and South Atlantic). Figure 7, highlights that the tropical mean response is not representative of regional responses. Figure 6 highlights the fact that the mechanisms for the changes in precipitation are region specific. Hence, each region has to must be

studied separately to understand the physical mechanism that caused the changes in (P-E). Of particular interest is the Indian monsoon. Both BoB and Indian landmass $P - E$. Both the Indian land mass and the Bay of Bengal are part of this monsoon the Indian monsoon system, yet they have opposite response to demonstrate a different response to the precessional forcing. Hence, we discuss this asymmetric response of Indian monsoon in detail, in detail in the following subsection. Such an asymmetry also exists within the East Asian monsoon, which has been discussed in a separate subsection.

4.2 The Indian monsoon

From figure 7a, we have established that the increase and decrease of (P-E) over India and BoB respectively was due to Q_{div} . Here we examine in detail, what caused these changes in Q_{div} . We look at each of the fluxes at the surface and Top of Atmosphere (TOA) separately:-

$$Q_{div} = \underbrace{LHF + SHF + Net_Sfc_Rad}_{\text{bottom fluxes}} + \underbrace{Net_TOA_LW + Net_TOA_SW}_{\text{TOA Fluxes}}$$

Where, LHF : Surface Latent Heat Flux SHF : Surface Sensible Heat Flux Net_Sfc_Rad = Net Surface Radiation (Long wave + Short wave) Net_TOA_LW : Net Top Of Atmosphere Long wave radiation Net_TOA_SW : Net Top Of Atmosphere Short wave radiation

Clubbing together all the radiation fluxes into one quantity Q_{rad} , we get:-

$$Q_{div} = LHF + SHF + Q_{rad}$$

Figure 8, Battisti et al. (2014) suggested that different response of the Indian land mass and the Bay of Bengal is due to migration of near-surface equivalent potential temperature from the Bay of Bengal over to India. This is because the rate of increase in insolation is higher in the high insolation (similar to P_{min}) experiment. This causes the equivalent potential temperature θ_e to rise rapidly over India. It is known that the location of ITCZ coincides with that of the surface energy maxima (Bordoni and Schneider, 2008; ?). Hence ITCZ migrates over India quickly and remains there. However, EC-Earth simulates higher near-surface equivalent potential temperature θ_e over the Bay of Bengal, in both P_{min} and P_{max} (Fig. 7). In this section, we propose an alternate mechanism for the different response of the Indian land mass and the Bay of Bengal to the changes in precession.

We had argued earlier that while there was an increase in Q_{div} over the Indian land mass, there was a decrease in Q_{div} over the Bay of Bengal. (Fig. 6). Here we examine the factors that caused the changes in Q_{div} . Splitting Q_{div} into its component fluxes (Eq. 5) will help us to determine which flux contributed the most. Figure 8 is a spatial map of the differences in (P-E), Q_{div} and its components. Q_{div} , $P - E$, Q_{div} and its component fluxes Q_{rad} , LHF, and SHF. Q_{div} has a good spatial coherence with (P-E) $P - E$, over most of the regions except Arabian sea the Arabian Sea. As was discussed earlier, this is due to the changes in TGMS drive the changes in (P-E) over Arabian sea. Also note that (P-E), which is able to counter the effect of

reduced Q_{div} . $P - E$ has decreased along the southern parts of the western ghats, Western Ghats but has increased in the northern extent parts of the Western Ghats. Q_{rad} bears a better resemblance to $(P - E)$. Q_{rad} bears a resemblance to $P - E$. This suggests that radiative feedbacks from clouds are present. But these feedbacks are not able to counter the large decrease in Latent Heat Flux (LHF) over Arabian sea and BoB. This makes Q_{div} decrease the Arabian Sea and the Bay of Bengal. Thus, the decrease in LHF over these regions reduces Q_{div} there. In fact Q_{div} , Q_{div} and LHF have similar spatial patterns over the oceanic regions. The changes in Sensible Heat Fluxes-Flux (SHF) are small in most places.

To establish quantitatively, what drives changes in Q_{div} , we take two regions one over Central India (15° - 25° N; 73° - 83° E) : one over central India and the other over BoB (10° - 20° N; 85° - 95° E) the Bay of Bengal, to identify the flux which contributes most to the changes in Q_{div} . These regions are shown as outlined with black boxes in Figure 8a. The changes in the three components of Q_{div} , Q_{div} over these two regions is shown in the bar chart (Figure 8f) are depicted in the bar chart (Fig. 8f). It shows the dominance of the radiative terms over India, and LHF over BoB the Bay of Bengal, respectively.

LHF is a function of surface wind speed, Sea Surface Temperature (SST) and how close the atmosphere is to saturation near surface relative humidity. LHF increases with increase in wind speed and SST. However, an increase in SST and wind speed. SST has increased over BoB the Bay of Bengal and Southern Arabian sea-Sea by about 2° C (not shown). Supplementary figure S1). Thus, it cannot explain the decrease in LHF. Hence, we look at the changes in wind speed (Figure 9 Fig. 9). The top panel of Figure 9 Fig. 9 (a and b) show the JJA-mean winds at 850 hPa. The shading indicates wind speed and the unit vectors the direction streamlines show the direction of flow. The axis of the Low Level Jet low-level jet (LLJ) has shifted to the north and this has caused led to a decrease in winds over BoB the Bay of Bengal. Due to LLJ, deep oceanic water upwells along the coast of Somalia. This makes the SST over leads to cooler SSTs over the western parts of Arabian sea colder. However, due to the northward shift of the LLJ the Arabian Sea. Since in P_{min} , LLJ has shifted further north, the region of upwelling also shifts north. Thus, leading to cooler SSTs in the Northern Arabian sea. Thus the decrease in LHF over Arabian sea is west coast of northern Arabian Sea (Supplementary figure S1). Hence, LHF over the Arabian Sea decreases due to weaker winds in the southern parts and colder SST in the northern parts.

Also the The shift in LLJ leads to lesser moisture flux along the southern part of the Western Ghats. Hence, the decrease in $(P - E)$ $P - E$ decreases there. At the same time the LLJ now, the LLJ brings more moisture into the northern parts of the Western Ghats, leading to increase in $(P - E)$ $P - E$. The shift of the LLJ can be seen more clearly in Figure 9c, where the difference in winds between P_{min} and P_{max} is shown. There is a low level easterly along the equatorial Indian ocean and a low level westerly over the African landmass, also along the equator. These two low level winds converge near the eastern coast of Along the equator, there exists an anomalous low-level easterly over the Indian Ocean. This meets an anomalous westerly from over the equatorial Africa, at around longitude 40° E. Also This indicates low-level convergence. Furthermore, on the same meridian is meridian, there exists a cyclonic circulation to the north, situated (over the Middle-East) and an anti-cyclonic circulation to the south, over Madagasear (over Madagascar). This resembles the Gill-like response of the atmosphere to winds to the heating of an atmospheric column (Gill, 1980) as shown by Gill (1980).

(Gill, 1980) Gill (1980) proposed a simple shallow water model on an equatorial β plane to ~~understand~~ elucidate the role of latent heating on surface winds. ~~He put heat sources in different regions, to heat the entire atmospheric column over these regions. This was meant to~~ In order to represent convective heating due to latent heat release, he introduced mass divergence in the atmospheric column. When this model was forced with ~~heating~~ "heating" over a region at the equator and another region ~~off-equator~~ to the north of the equator, it produced a Kelvin wave ~~along the equator and a Mixed Rossby-Gravity wave~~ which had a cyclonic and an anti-cyclonic circulation in the northern hemisphere and southern hemisphere respectively. The Kelvin wave causes low level convergence along and a mixed Rossby-gravity wave. The Kelvin wave leads to an anomalous low-level easterly and an anomalous low-level westerly along the equator. The easterly is to the east of the heat source and the westerly to the west of the heat source. These anomalous winds thus lead to low-level convergence at the equator, over near the region of ~~equatorial~~ the heat source. The mixed Rossby-gravity wave has a cyclonic circulation to the north of the equator and an anti-cyclonic circulation to the south of the equator. The wind response of ~~our model, hence~~ EC-Earth hence, suggests that the wind patterns over the Indian subcontinent, are driven by atmospheric heating near the equator and off-equator ~~and off-equator~~. Examining figure ~~6a, will show~~ 5a shows that the heat sources correspond to convective heating of the column due to increased precipitation over the West Equatorial Indian Ocean (WEIO) and over the ~~Red sea. The convection over the Red sea, is part of the African monsoon which has extended into this region~~ Middle-East (particularly the Red Sea). There are, however, some important differences between ~~our model~~ EC-Earth and the Gill model. ~~Ours~~ EC-Earth is a full GCM with non-zero mean background winds, whereas Gill model ~~has~~ is linearized with respect to zero mean background winds. ~~This implies that our model~~ Thus, the EC-Earth's response includes non-linear terms as well.

To summarize, the decrease in ~~Q_{div} over BoB,~~ Q_{div} over the Bay of Bengal is due to ~~decreased winds over BoB~~ lower wind speeds. The winds decrease ~~on account of a remote response to~~ because of convective heating over WEIO west equatorial Indian Ocean and the Red Sea. The ~~next question we want to address is,~~ what factors lead to increased convection convection over the Red Sea is an extension of the African monsoon. Hence, we examine the factors which lead to an increase in precipitation over these regions. To understand this, we look at the The prevailing conditions in the pre-monsoon month of May, even before the Indian monsoon circulation has set up. Figure 10a leads to enhanced convection over these regions, later in the summer. Figure 10a and b, show the difference in ~~Q_{div} and $(P-E)$~~ Q_{div} and $P-E$ for the month of May. ~~The shading in figure 10b is for $(P-E)$ and the unit vectors~~ Figure 10b shows changes in $P-E$ in shading and the streamlines represent the changes in the wind direction. ~~Q_{div}~~ Q_{div} is higher over Africa, and this causes early onset of ~~monsoon~~ (Figure 10b). ~~Thus changing the low~~ the African monsoon (Fig. 10b) and changes the low-level winds along the eastern coast of Africa. This leads to reduced upwelling and increased SST. With increased SST, convection begins and this further enhances the low The SST along the eastern coast depends on the coastal upwelling. The changes in winds thus reduce upwelling and increase SST. This enhances convection over the west equatorial Indian Ocean, further leading to low-level convergence. This positive feedback is responsible for the convective heating ~~over the WEIO~~ that persists through the summer months. As the African monsoon progresses north, the season advances from May onwards, the African monsoon propagates northward. The region of convection over the eastern side of Africa moves over to the Red ~~sea~~ Sea. This becomes the off-equatorial heat source.

4.3 The South East Asian monsoon

Shi et al. (2012) showed that the South East Asian monsoon and the North East Asian monsoon are out of phase owing to the El-Nino like SST pattern in P_{\min} . Here we are addressing the differences in the precipitation changes over South East Asia (land) and the adjacent ocean. The domain for South East Asia is shown in figure 8b. Based on the analysis using Eq. 15, we find that the increase (decrease) in $P - E$ over the land (ocean) grids is mainly due to the increase (decrease) in Q_{div} (Fig. 6). Even though Q_{div} is dominant, the contribution of TGMS is higher over the SE Asia (oceanic regions) when compared to the Bay of Bengal. Once again decomposing Q_{div} into its component fluxes suggests a similar mechanism that leads to the India–Bay of Bengal redistribution of precipitation (Fig. 8f). The increase in insolation leads to an increase in Q_{div} over the SE Asian land, whereas a decrease in LHF over the oceanic regions leads to a decrease in Q_{div} . The convective heating over WEIO and the Red Sea leads to reduced winds, and hence decreased LHF in the North West Pacific.

5 Discussion and conclusions

In this section, we have summarized our results and have discussed the similarities between the sets of idealized experiments (P_{\min} , P_{\max}) vs (Mid-Holocene (MH), Pre-Industrial (PI)). The MH and PI experiments were conducted with the same model EC-Earth, the details of which are available in Bosmans et al. (2012). The difference in solar forcing between MH and PI is similar to that between P_{\min} and P_{\max} , albeit with a smaller amplitude (Supplementary figure S2). Moreover, MH has an obliquity 0.66° higher than PI, and hence it contributes little to the total forcing (Supplementary figure S2b). Previous research with models has shown that the climate response to precession is independent of obliquity (Tuenter et al., 2003). The climate of MH is therefore mainly driven by precession. The peak in the insolation difference between MH and PI is delayed by a month with respect to the insolation difference between P_{\min} and P_{\max} . Hence the largest precipitation changes in MH occur about a month later than in P_{\min} (Fig. 4 and supplementary figure S3). Therefore, we consider Jul–Aug–Sep averages for MH. The land–ocean shift in precipitation in MH is qualitatively explained by changes in Q_{div} (supplementary figure S4). Particularly, the displacement of precipitation from the Bay of Bengal to India is due to the same mechanism that drives these changes in P_{\min} (Supplementary figures S5, S6, and S7). The SE Asian monsoon also exhibits a land–ocean shift in rainfall. This is due to radiative heating over land as well as the ocean. This suggests that the cloud radiative feedbacks are stronger for the SE Asian monsoon. The changes in LHF are, however, due to the same reason as in P_{\min} . We repeated the analysis for a set of obliquity experiments T_{\max} and T_{\min} , corresponding to the maximum and minimum tilt, with eccentricity set to zero (Bosmans et al., 2015). The tropical precipitation shows a land–ocean shift in precipitation, but the amplitude of change is small compared to the precession experiments (Supplementary figure S9). The mechanisms leading to this shift are different for obliquity and precession (Supplementary figures S10 and S11).

Models with different levels of complexities: QTCM (Hsu et al., 2010), Quasi-geostrophic model EC-Bilt (Tuenter et al., 2003), GCM with slab ocean (Battisti et al., 2014) and finally the fully coupled model EC-Earth (Bosmans et al., 2018) ; have all shown ~~the land-sea asymmetry in precipitation~~ a shift in precipitation between land and ocean, when subjected to the precessional forcing. ~~Also the land-sea asymmetry exists irrespective of the details of the orbital configuration (Mid-holocene,~~

or idealized experiments). This suggests that the asymmetry is on account of a very fundamental mechanism. We agree with the previous studies that this is on account of the *slow ocean response*. However, changes in precipitation over ocean are not of the same sign everywhere (Figure 6a). In fact ocean has a more heterogeneous response than land, suggesting that the role of local processes dominates over the slow ocean response in these regions. Hence, it is necessary to study smaller regions, separately to understand the precipitation response (Figure 7) there are no proxies for precipitation over oceans to verify this. Since the climate over islands is influenced by the surrounding oceans, proxies obtained from islands can be thought of as a representation of climate over the surrounding ocean. A speleothem chronology from the Baratang cave in the Andaman Islands (Laskar et al., 2013) in this regard, represents precipitation over the Bay of Bengal. This chronology goes back to 4,000 years before present and shows a long-term decreasing trend in precipitation as we move back in time. The time period corresponding to 4 ka being closer to MH has higher summer insolation and proxies over Indian continent register an increase in precipitation (Ramesh, 2001; Patnaik et al., 2012; Zhang et al., 2016; Kathayat et al., 2017). This suggests that the GCMs and observations indicate the response of Indian land mass is different from the response in the Bay of Bengal.

~~We have analysed and~~ Using a simple model for ITCZ, we have interpreted the response of a high resolution fully coupled model EC-Earth, ~~to precession, by using a simple model, based on the conservations of energy and moisture. With the help of the simple model, we can diagnose the~~ to precession. The changes in precipitation, ~~in terms of two variables, viz. the total energy can be attributed to either the changes in total energy fluxes~~ going into the column (Q_{div}) ~~and the Q_{div}~~ or the changes in vertical stability of the atmosphere ($GMSTGMS$). We have included the horizontal advection terms in the calculation of TGMS, which were originally assumed to be small (Neelin and Held, 1987). This allows us to use the simple ITCZ model for relatively smaller domains, where horizontal advection terms can be large. ~~We~~ TGMS represents the total transport of the MSE. In places where the horizontal transport is weak, TGMS is the same as GMS. Changes in precession provide an initial forcing. The final response of the precipitation is due to this initial forcing and the consequent feedbacks. These feedbacks are in the form changes in surface energy fluxes and changes in stability of the atmosphere. In agreement with Chamales (2014), we find that precipitation changes between precession extremes, ~~are in general~~ over the whole tropics are, due to changes in Q_{div} . ~~Insolation Q_{div}~~ over land and due to TGMS over the ocean. This generalization is, however, not valid for smaller regions. Within the domain of the South Asian monsoon, insolation drives changes in Q_{div} over Q_{div} over the land, whereas latent heat fluxes contribute most over the oceans. Particularly, the ~~changes in winds decrease in LHF~~ over the Bay of Bengal, ~~cause latent heat fluxes to decrease~~ and the North-West Pacific is associated with the weakening of the low-level westerlies over these regions. These changes in ~~wind speed are associated with convecting westerlies~~ are driven by convective heating of the atmospheric column over the ~~west equatorial Indian ocean and the Red sea~~.

~~EC-Earth does get an increase in precipitation over the Indian landmass for minimum precession (higher summer insolation), consistent with the proxy records (Kathayat et al., 2017). However, there are no proxies for precipitation over oceanic regions. As we move further back in time (through the Holocene), we move closer to a minimum precession configuration. This means higher summer insolation and lower winter insolation than the present day. Hence, we would expect precipitation to decrease over the Bay of Bengal as we move further back in time, through the Holocene. A speleothem chronology from the Baratang cave in the Andaman islands (Laskar et al., 2013), can be thought of as a representation of precipitaion over the Bay. This~~

chronology goes back to 4 western equatorial Indian Ocean and the Middle-east. There are, 000 years before present, and shows a long-term decreasing trend in precipitation. This suggests that the EC-Earth is doing well in capturing the land-sea asymmetry between India and Bay of Bengal.

5 There are however, regions where changes in stability the changes in TGMS is the main cause of the changes in precipitation (eg.e.g., Africa and Arabian sea). Stability (the Gross Moist Stability) is based on the coupling between the divergence of moisture and moist static energy fluxes. This suggests that between the precession extremes, this coupling had changed. Why it changes so, requires further investigation.

6

10 For orbital configuration with higher summer insolation, the rate of increase in surface temperature is high over India (due to lower thermal heat capacity). Battisti et al. (2014) suggested that this causes near surface MSE to be higher over India. It is known that the location of ITCZ coincides with that of the surface MSE (Bordoni and Schneider, 2008). Hence ITCZ migrates over India quickly and remains there. However, our plot of near surface equivalent potential temperature, θ_e (same as near surface MSE), suggests that BoB has higher energy all throughout the year for both the precession extremes (Figure A1) We have demonstrated that the simple ITCZ model can be used to explain the precipitation response for any orbital configuration
15 (e.g., MH, maximum and minimum obliquity experiments).

Author contributions. C. Jalihal, J. Srinivasan and A. Chakraborty analysed and interpreted the GCM output. J.H.C Bosmans designed and ran the experiments. C. Jalihal wrote the manuscript with input from all authors. All authors reviewed the manuscript.

Competing interests. The authors declare that they have no conflict of interest.

Acknowledgements. We thank A. Nikumbh for useful comments. The authors acknowledge support from the Centre for Excellence in the
20 Divecha Centre for Climate Change (DCCC). This work was partially funded by DST India.

References

- Balsamo, G., Beljaars, A., Scipal, K., Viterbo, P., van den Hurk, B., Hirschi, M., and Betts, A. K.: A revised hydrology for the ECMWF model: Verification from field site to terrestrial water storage and impact in the Integrated Forecast System, *Journal of hydrometeorology*, 10, 623–643, 2009.
- 5 Battisti et al.: Coherent pan-Asian climatic and isotopic response to orbital forcing of tropical insolation, *Journal of Geophysical Research: Atmospheres*, 119, 2014.
- Bechtold, P., Köhler, M., Jung, T., Doblas-Reyes, F., Leutbecher, M., Rodwell, M. J., Vitart, F., and Balsamo, G.: Advances in simulating atmospheric variability with the ECMWF model: From synoptic to decadal time-scales, *Quarterly Journal of the Royal Meteorological Society*, 134, 1337–1351, 2008.
- 10 Berger, A.: Long-term variations of daily insolation and Quaternary climatic changes, *Journal of the Atmospheric Sciences*, 35, 2362–2367, 1978.
- Bordoni, S. and Schneider, T.: Monsoons as eddy-mediated regime transitions of the tropical overturning circulation, *Nature Geoscience*, 1, 515, 2008.
- Bosmans et al.: Monsoonal response to mid-holocene orbital forcing in a high resolution GCM, *Climate of the Past*, 8, 723, 2012.
- 15 Bosmans, J., Drijfhout, S., Tuenter, E., Hilgen, F., and Lourens, L.: Response of the North African summer monsoon to precession and obliquity forcings in the EC-Earth GCM, *Climate dynamics*, 44, 279–297, 2015.
- Bosmans, J., Erb, M., Dolan, A., Drijfhout, S., Tuenter, E., Hilgen, F., Edge, D., Pope, J., and Lourens, L.: Response of the Asian summer monsoons to idealized precession and obliquity forcing in a set of GCMs, *Quaternary Science Reviews*, 188, 121–135, 2018.
- Braconnot et al.: Ocean feedback in response to 6 kyr BP insolation, *Journal of Climate*, 13, 1537–1553, 2000.
- 20 Braconnot et al.: Monsoon response to changes in Earth’s orbital parameters: comparisons between simulations of the Eemian and of the Holocene, *Climate of the Past Discussions*, 4, 459–493, 2008.
- Caley, T., Roche, D. M., and Renssen, H.: Orbital Asian summer monsoon dynamics revealed using an isotope-enabled global climate model, *Nature communications*, 5, 5371, 2014.
- Chamales, K. A.: The effects of orbital precession on tropical precipitation, 2014.
- 25 Chou, C. and Neelin, J. D.: Mechanisms of global warming impacts on regional tropical precipitation, *Journal of climate*, 17, 2688–2701, 2004.
- Chou, C., Neelin, J. D., Lohmann, U., and Feichter, J.: Local and remote impacts of aerosol climate forcing on tropical precipitation, *Journal of climate*, 18, 4621–4636, 2005.
- Chou, C., Neelin, J. D., Tu, J.-Y., and Chen, C.-T.: Regional tropical precipitation change mechanisms in ECHAM4/OPYC3 under global warming, *Journal of Climate*, 19, 4207–4223, 2006.
- 30 Clement, A. C., Hall, A., and Broccoli, A.: The importance of precessional signals in the tropical climate, *Climate Dynamics*, 22, 327–341, 2004.
- Cruz Jr, F. W., Burns, S. J., Karmann, I., Sharp, W. D., Vuille, M., Cardoso, A. O., Ferrari, J. A., Dias, P. L. S., and Viana Jr, O.: Insolation-driven changes in atmospheric circulation over the past 116,000 years in subtropical Brazil, *Nature*, 434, 63, 2005.
- 35 Donohoe, A., Marshall, J., Ferreira, D., and Mcgee, D.: The relationship between ITCZ location and cross-equatorial atmospheric heat transport: From the seasonal cycle to the Last Glacial Maximum, *Journal of Climate*, 26, 3597–3618, 2013.
- Gadgil, S.: The monsoon system: Land–sea breeze or the ITCZ?, *Journal of Earth System Science*, 127, 5, 2018.

- Gill, A.: Some simple solutions for heat-induced tropical circulation, *Quarterly Journal of the Royal Meteorological Society*, 106, 447–462, 1980.
- Hazeleger, W., Severijns, C., Semmler, T., Ștefănescu, S., Yang, S., Wang, X., Wyser, K., Dutra, E., Baldasano, J. M., Bintanja, R., et al.: EC-Earth: a seamless earth-system prediction approach in action, *Bulletin of the American Meteorological Society*, 91, 1357–1363, 2010.
- 5 Hazeleger, W., Wang, X., Severijns, C., Ștefănescu, S., Bintanja, R., Sterl, A., Wyser, K., Semmler, T., Yang, S., Van den Hurk, B., et al.: EC-Earth V2. 2: description and validation of a new seamless earth system prediction model, *Climate dynamics*, 39, 2611–2629, 2012.
- Hsu et al.: Land–ocean asymmetry of tropical precipitation changes in the mid-Holocene, *Journal of Climate*, 23, 4133–4151, 2010.
- Kang, S. M., Held, I. M., Frierson, D. M. W., and Zhao, M.: The Response of the ITCZ to Extratropical Thermal Forcing: Idealized Slab-Ocean Experiments with a GCM, *Journal of Climate*, 21, 3521–3532, <https://doi.org/10.1175/2007JCLI2146.1>, <https://doi.org/10.1175/2007JCLI2146.1>, 2008.
- 10 Kathayat, G., Cheng, H., Sinha, A., Yi, L., Li, X., Zhang, H., Li, H., Ning, Y., and Edwards, R. L.: The Indian monsoon variability and civilization changes in the Indian subcontinent, *Science advances*, 3, e1701 296, 2017.
- Kutzbach, J., Liu, X., Liu, Z., and Chen, G.: Simulation of the evolutionary response of global summer monsoons to orbital forcing over the past 280,000 years, *Climate Dynamics*, 30, 567–579, 2008.
- 15 Kutzbach, J. E.: Monsoon climate of the early Holocene: climate experiment with the earth’s orbital parameters for 9000 years ago, *science*, 214, 59–61, 1981.
- Laskar, A. H., Yadava, M., Ramesh, R., Polyak, V., and Asmerom, Y.: A 4 kyr stalagmite oxygen isotopic record of the past Indian Summer Monsoon in the Andaman Islands, *Geochemistry, Geophysics, Geosystems*, 14, 3555–3566, 2013.
- Madec, G.: NEMO, the ocean engine, Note du Pole de modelisation, Institut Pierre-Simon Laplace (IPSL), France, No 27 ISSN No 1288–1619, 2008.
- 20 Merlis et al.: Hadley circulation response to orbital precession. Part II: Subtropical continent, *Journal of Climate*, 26, 754–771, 2013.
- Mohtadi, M., Prange, M., and Steinke, S.: Palaeoclimatic insights into forcing and response of monsoon rainfall, *Nature*, 533, 191, 2016.
- Neelin, J. D. and Held, I. M.: Modeling tropical convergence based on the moist static energy budget, *Monthly Weather Review*, 115, 3–12, 1987.
- 25 Patnaik et al.: Indian monsoon variability at different time scales: marine and terrestrial proxy records, 2012.
- Pokras, E. M. and Mix, A. C.: Earth’s precession cycle and Quaternary climatic change in tropical Africa, *Nature*, 326, 486–487, 1987.
- Ramesh, R.: High resolution Holocene monsoon records from different proxies: An assessment of their consistency, *Current Science*, pp. 1432–1436, 2001.
- Schneider, T., Bischoff, T., and Haug, G. H.: Migrations and dynamics of the intertropical convergence zone, *Nature*, 513, 45, 2014.
- 30 Shi, Z.: Response of Asian summer monsoon duration to orbital forcing under glacial and interglacial conditions: Implication for precipitation variability in geological records, *Quaternary Science Reviews*, 139, 30–42, 2016.
- Shi, Z., Liu, X., and Cheng, X.: Anti-phased response of northern and southern East Asian summer precipitation to ENSO modulation of orbital forcing, *Quaternary Science Reviews*, 40, 30–38, 2012.
- Sterl, A., Bintanja, R., Brodeau, L., Gleeson, E., Koenigk, T., Schmith, T., Semmler, T., Severijns, C., Wyser, K., and Yang, S.: A look at the ocean in the EC-Earth climate model, *Climate Dynamics*, 39, 2631–2657, 2012.
- 35 Tuenter et al.: The response of the African summer monsoon to remote and local forcing due to precession and obliquity, *Global and Planetary Change*, 36, 219–235, 2003.

- Tuenter, E., Weber, S., Hilgen, F., Lourens, L., and Ganopolski, A.: Simulation of climate phase lags in response to precession and obliquity forcing and the role of vegetation, *Climate Dynamics*, 24, 279–295, 2005.
- Valcke, S. and Morel, T.: OASIS and PALM, the CERFACS couplers, Tech. rep., Tech. rep., CERFACS, 2006.
- Wang et al.: Millennial-and orbital-scale changes in the East Asian monsoon over the past 224,000 years, *Nature*, 451, 1090–1093, 2008.
- 5 Wang, X., Auler, A. S., Edwards, R., Cheng, H., Ito, E., Wang, Y., Kong, X., and Solheid, M.: Millennial-scale precipitation changes in southern Brazil over the past 90,000 years, *Geophysical Research Letters*, 34, 2007.
- Weber, S. and Tuenter, E.: The impact of varying ice sheets and greenhouse gases on the intensity and timing of boreal summer monsoons, *Quaternary Science Reviews*, 30, 469–479, 2011.
- Zhang et al.: Holocene Asian monsoon evolution revealed by a pollen record from an alpine lake on the southeastern margin of the Qinghai–
10 Tibetan Plateau, China, *Climate of the Past*, 12, 415–427, 2016.
- Zhao, Y. and Harrison, S.: Mid-Holocene monsoons: a multi-model analysis of the inter-hemispheric differences in the responses to orbital forcing and ocean feedbacks, *Climate Dynamics*, 39, 1457–1487, 2012.

Table 1. The orbital configuration used for the extremes in precession, Precession minima: P_{\min} , Precession maxima: P_{\max} and the ~~pre-industrial~~pre- industrial. ‘e’ represents eccentricity, δ is the tilt and ω is the longitude of perihelion. The values of these have been chosen, based on the extremes in the precession parameter $e \sin(\pi + \omega)$ ~~$e * \sin(\pi + \omega)$~~ , that have occurred in the last 1 Myrs Berger (1978). Pre-industrial values are shown for comparison.

	<u>Eccentricity, e</u>	<u>δ ($^{\circ}$) Obliquity, δ ($^{\circ}$)</u>	<u>ω ($^{\circ}$) Longitude of perihelion, ω ($^{\circ}$)</u>
Pre-Industrial	0.017	23.45	282.04
P_{\min}	0.056	22.08	95.96
P_{\max}	0.058	22.08	273.5

Table 2. This table lists all the The regions used in this article, and provides their corresponding co-ordinates their coordinates.

Region	Co-ordinates
Northern tropics	(0° N -30° <u>N</u> ; 0° E -360° <u>E</u>)
Southern tropics	(30° S -0° <u>N</u> ; 0° E -360° <u>E</u>)
Central India	(15° N -25° <u>N</u> ; 73° E -83° <u>E</u>)
Bay of Bengal	(10° N -20° <u>N</u> ; 85° E -95° <u>E</u>)
<u>South East Asia</u>	(0° <u>N</u> -25° <u>N</u> ; 100° <u>E</u> -125° <u>E</u>)
Arabian Sea	(5 10° N -20° <u>N</u> ; 60° E -70° <u>E</u>)
N. Africa	(5° N -15° <u>N</u> ; 20° W -0° <u>E</u>)
Brazil	(20° S -10° <u>S</u> ; 70° W -50° <u>W</u>)
South Atlantic	(20° S -10° <u>S</u> ; 30° W -0° <u>E</u>)
South Africa	(20° S -10° <u>S</u> ; 15° E -35° <u>E</u>)
North Australia	(25° S -15° <u>S</u> ; 130° E -140° <u>E</u>)

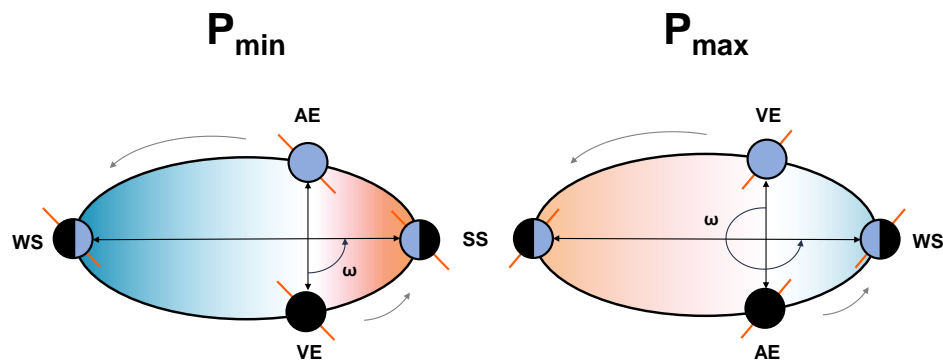


Figure 1. The schematic shows diagram showing the orbital configuration of minimum precession (P_{\min}) and maximum precession (P_{\max}). In P_{\min} , summer solstice (SS) takes place occurs at perihelion, while in P_{\max} , winter solstice (WS) coincides with the perihelion. AE and VE are the Autumn and Vernal Equinoxes equinoxes respectively.

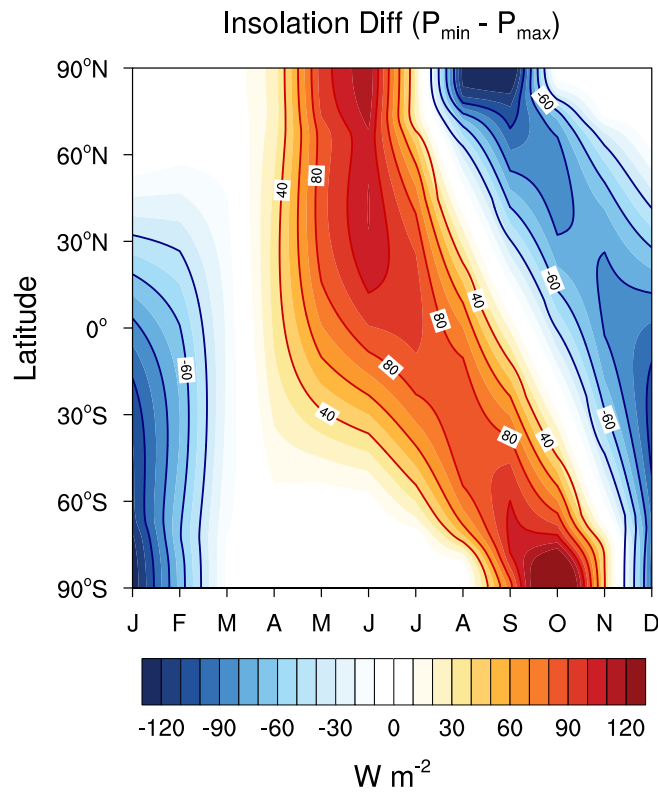


Figure 2. The difference in the incoming solar radiation at the top of atmosphere between P_{\min} and P_{\max} as a function of latitude and month. This shows that insolation in P_{\min} is higher during northern summer and lower during in the northern winter in P_{\min} hemisphere summer compared to P_{\max} .

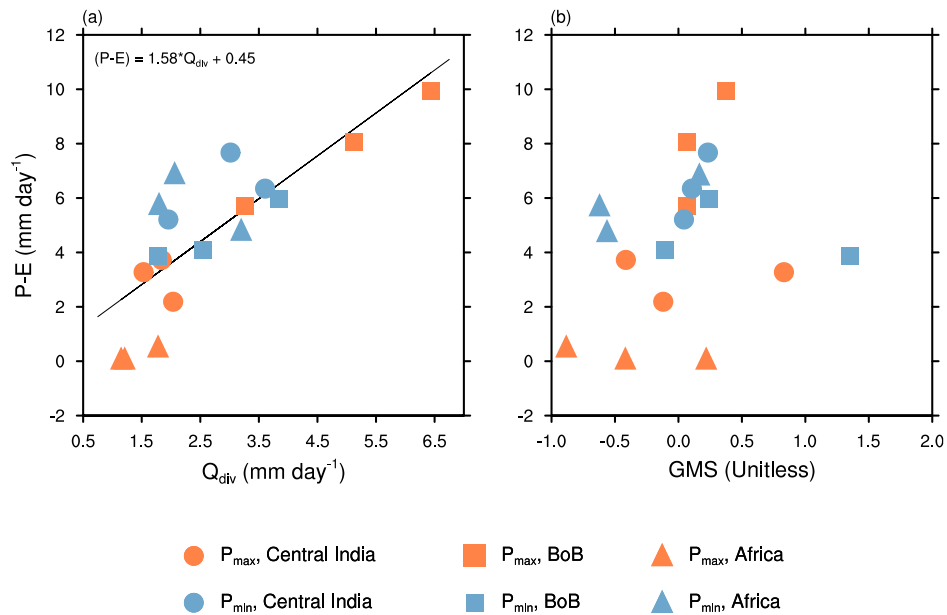


Figure 3. This figure shows the dependence of (P-E) on Q_{div} , (a) Q_{div} and (b) GMS, for three regions: Central India ($15^{\circ}\text{N}-25^{\circ}\text{N}$ - 25°N ; $73^{\circ}\text{E}-83^{\circ}\text{E}$ - 83°E), Bay of Bengal ($10^{\circ}\text{N}-20^{\circ}\text{N}$ - 20°N ; $85^{\circ}\text{E}-95^{\circ}\text{E}$ - 95°E) and Africa ($5^{\circ}\text{N}-15^{\circ}\text{N}$ - 15°N ; $20^{\circ}\text{W}-25^{\circ}\text{W}$ - 0°E). The scatter has been made for months Jun-Jul-Aug are taken separately. The hollow blue and filled orange symbols correspond to P_{max} and P_{min} respectively. (P-E) is directly proportional to Q_{div} . Same as figure (5), except that the x-axis is GMS. Negative values of GMS indicates that advection terms, which had have been neglected, are significant large.

The difference in precipitation ($P_{\min}-P_{\max}$) for tropical land and ocean taken separately ($30^{\circ}\text{S}-30^{\circ}\text{N}$). This shows the asymmetric response of the land and oceans to precessional forcing.

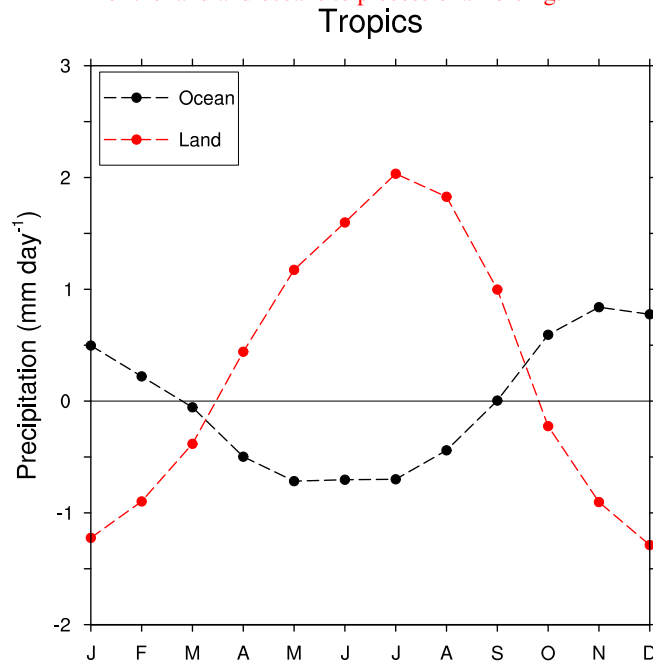


Figure 4. The figure shows difference in precipitation ($P-E$, $P_{\min}-P_{\max}$) (top panels (a) for all the tropical land and (e)) and Q_{div} ocean taken separately (bottom panels (b) and (d)) $30^{\circ}\text{S}-30^{\circ}\text{N}$. The left panels are for JJA and This shows the right panels for DJF different response of the land and oceans to precessional forcing.

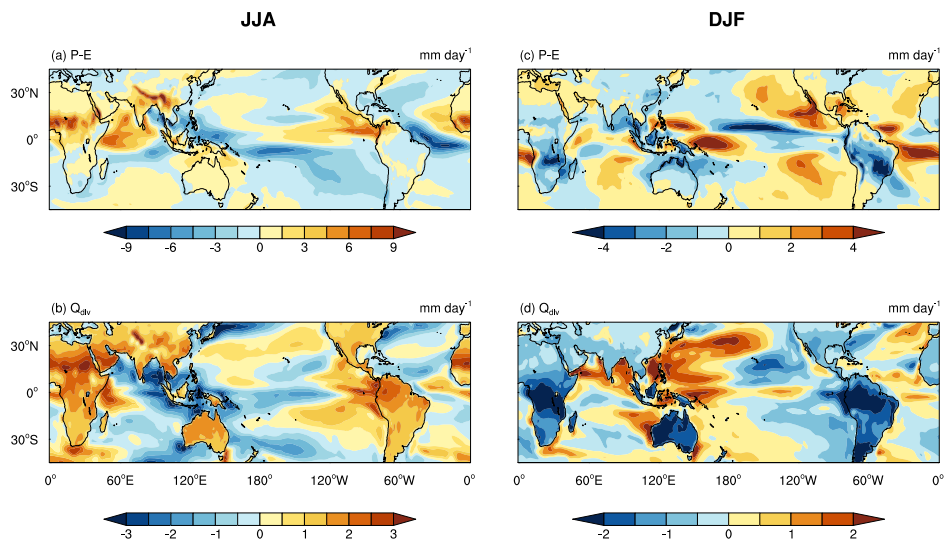


Figure 5. The difference in $P - E$ (top panel (a) and (c)) and Q_{div} (bottom panel (b) and (d)). The left panel is for JJA mean and the right panel for DJF mean.

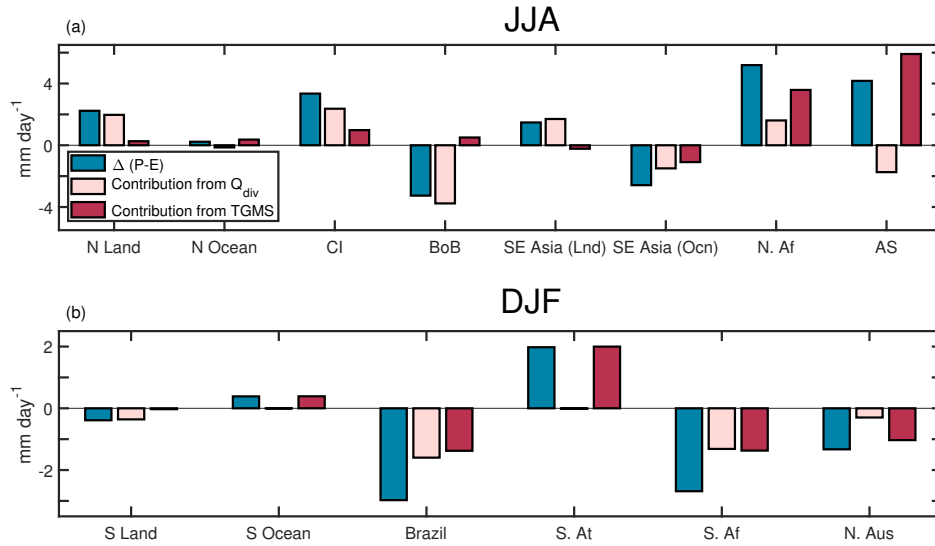


Figure 6. The bar chart shows the contribution of Q_{div} , Q_{div} and TGMS to the changes in $(P-E)P-E$. The top panel (a) is for the JJA mean and regions in the Northern Hemisphere, while the bottom panel (b) is for regions in the Southern Hemisphere and during-averaged over DJF. The blue stick bar is the change in $(P-E)P-E$, while red pink and orange sticks red bars represent the contribution from Q_{div} , Q_{div} and TGMS. The abbreviations used in the top panel (a), **N Land**: Northern tropics \div -(land only), **N Ocean**: Northern tropics \div -(Ocean only), **CI**: Central India, **BoB**: the Bay of Bengal, **ASSE Asia (Lnd)**: Arabian-sea-and-South East Asia (land only), **SE Asia (Ocn)**: South East Asia (Ocean only), **N. Af**: North Africa \div -and **AS**: Arabian Sea, and in the bottom panel (b), **S Land**: Southern tropics \div -(land only), **S Ocean**: Southern tropics \div -(ocean only), **S. At**: South Atlantic, **S. Af**: South Africa, **N. Aus**: North Australia. Refer to table 2 for the co-ordinates. The coordinates of these regions are provided in Table 2.

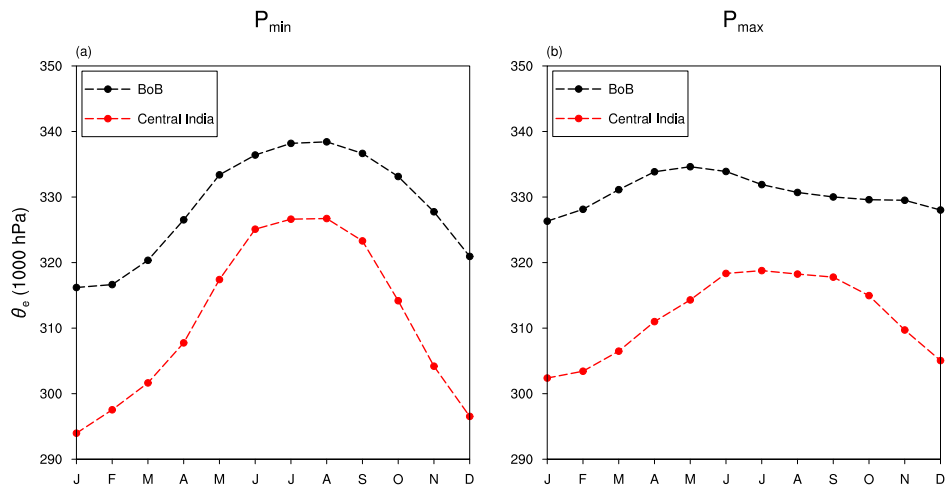


Figure 7. Shows The seasonal cycle of near-surface equivalent potential temperature (θ_e) over for India and the Bay of Bengal for, (a) P_{min} configuration, and (b) P_{max}

JJA

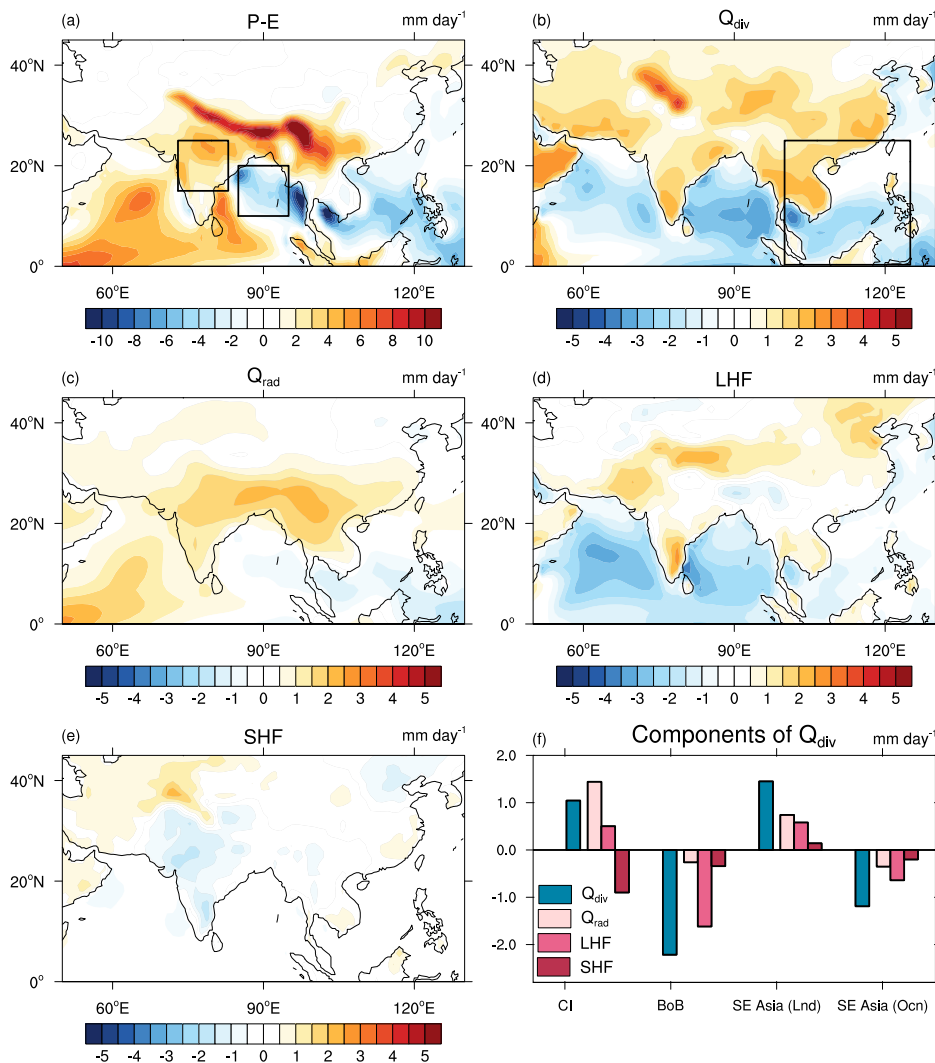


Figure 8. The JJA mean difference ($P_{\min}-P_{\max}$), in (a) $P-E$, (b) Q_{div} ($P-E$ sum of energy fluxes at the top and bottom of the atmosphere), (c) Q_{rad} (Q_{rad} (Sum of all radiative fluxes at the top and bottom of the atmosphere), (d) Latent Heat Fluxes heat flux, (e) Sensible Heat Fluxes heat flux. The two boxes shown in (a) and (b), are the regions chosen for this study: Central India ($15^{\circ}\text{N}-25^{\circ}\text{N}$; $73^{\circ}\text{E}-83^{\circ}\text{E}$) and Bay of Bengal ($10^{\circ}\text{N}-20^{\circ}\text{N}$; $85^{\circ}\text{E}-95^{\circ}\text{E}$) and South East Asia ($0^{\circ}\text{N}-25^{\circ}\text{N}$; $100^{\circ}\text{E}-125^{\circ}\text{E}$). (f) shows the decomposition of Q_{div} into radiative, latent and sensible heat fluxes for the two regions. The blue bar is the change in Q_{div} , red: change in Q_{rad} , orange: change in latent heat fluxes and purple: change in sensible heat fluxes.

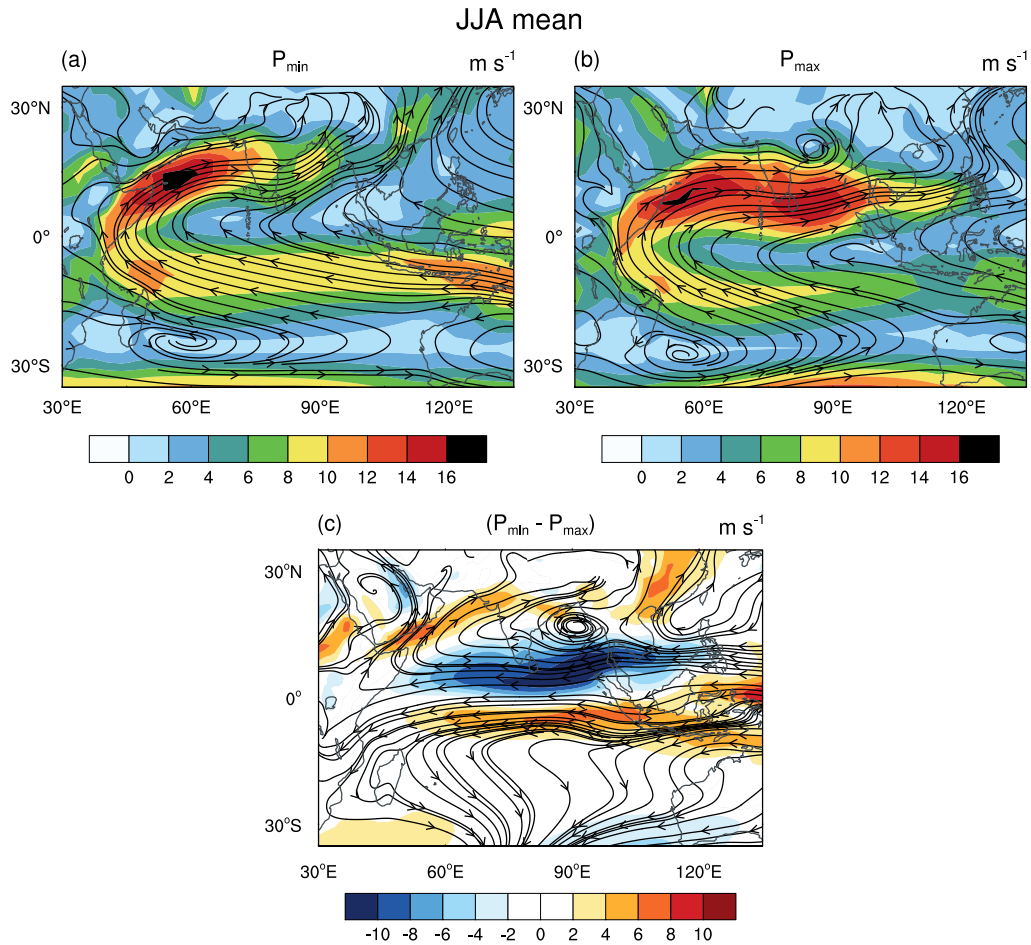


Figure 9. Top panels (a) and (a) show the The JJA mean windspeed wind speed (850 hPa) in shading with unit vectors indicating direction for (a) P_{min} and, (b) P_{max} respectively. The bottom panel (c), shows with streamlines of the wind vector field superimposed. The difference in of the winds (850 hPa). As can be seen from between P_{min} and P_{max} is shown in (c), 40°E longitude has a convergence at the equator and cyclonic circulation over the Middle-East. An anti-cyclonic circulation exists in the southern hemisphere over Madagascar. This is similar to the response of an the atmosphere to equatorial plus off-equatorial heating (Gill, 1980).

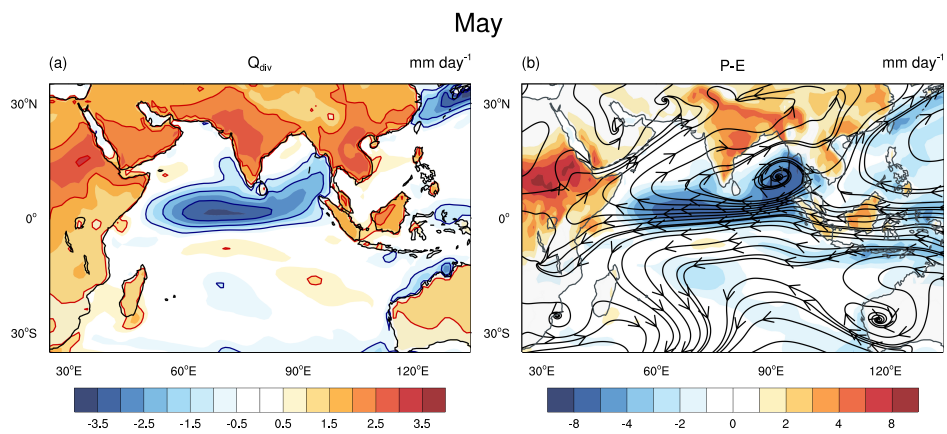


Figure 10. The difference between P_{min} and P_{max} in (a), Q_{div} and (b), $P-E$ along with unit vectors indicating streamlines of change in the wind direction, for the month of May. This shows that the large increase in Q_{div} over Africa causes leads to an early onset of African monsoon. Thus, influencing the winds over the equatorial Indian Ocean.

The plot shows the seasonal cycle of near-surface equivalent potential temperature for India and BoB in the, (a) P_{\min} configuration, and (b) P_{\max}